

CISPLATIN RELEASE CHARACTERISTICS FROM AMORPHOUS CALCIUM
POLYPHOSPHATE MATRICES FOR THE ADJUNCTIVE TREATMENT OF
ORAL SQUAMOUS CELL CARCINOMA

by

Matthew R Shaffner

Submitted in partial fulfilment of the requirements
for the degree of Master of Science

at

Dalhousie University
Halifax, Nova Scotia
March 2014

© Copyright by Matthew R Shaffner, 2014

DEDICATION

This work is dedicated to my wonderful wife Melanie, and my girls Maggie, Hallie and Scarlett, without whom, I do not think I would have had the strength to push through difficult times. My family has given me the freedom to chase my dreams and has always been there to welcome me home with open arms. I love you all very much.

M.

TABLE OF CONTENTS

LIST OF TABLES.....	v
LIST OF FIGURES.....	vi
ABSTRACT.....	viii
LIST OF ABBREVIATIONS USED.....	ix
ACKNOWLEDGMENTS.....	x
CHAPTER 1 INTRODUCTION.....	1
1.1 HEAD AND NECK SQUAMOUS CELL CARCINOMA.....	1
1.1.1 Stage I, II – Surgical Treatment.....	2
1.1.2 Stage III, IV – Multi-modal therapy.....	2
1.2 CHEMOTHERAPY.....	4
1.3 CISPLATIN.....	6
1.4 CISPLATIN AND SUSTAINED RELEASE COMPOUNDS.....	9
1.5 CALCIUM POLYPHOSPHATE.....	10
1.6 OBJECTIVES.....	13
CHAPTER 2 MATERIALS AND METHODS.....	16
2.1 MATRIX PREPARATION.....	16
2.2 DRUG LOADING AND G1 DISK PRODUCTION.....	17
2.3 G2 DISK AND PELLET FABRICATION.....	18
2.4 ELUTION PROTOCOL.....	20
2.5 CISPLATIN RELEASE MEASUREMENTS.....	21
2.6 MINIATURIZED ELUTION	21
2.7 CISPLATIN VIABILITY.....	22
2.8 STATISTICAL ANALYSIS.....	24
CHAPTER 3 RESULTS.....	25
3.1 DOSE DEPENDENT LOADING STUDY.....	25
3.2 ELUTION STUDY.....	26
3.3 CISPLATIN RELEASE.....	28

3.4	CPP MATRIX DENSITY.....	37
3.5	CISPLATIN ACTIVITY.....	38
CHAPTER 4 DISCUSSION.....		41
4.1	CISPLATIN LOADING INTO CPP MATRIX.....	41
4.2	DRUG ELUTION.....	43
4.3	CISPLATIN ACTIVITY.....	47
4.4	CLINICAL RELEVANCE AND APPLICATION.....	49
CHAPTER 5 LIMITATIONS AND FUTURE WORK.....		51
5.1	LIMITATIONS.....	51
5.2	FUTURE WORK.....	52
CHAPTER 6 CONCLUSION		53
BIBLIOGRAPHY.....		54

LIST OF TABLES

Table 1	Dose dependent loading of a fully saturated cisplatin solution vs. the saturated solution diluted by 50%_	25
Table 2	Density of axial pressed disks and CIP processed pellets_	37
Table 3	MTT assay results comparing both positive control and test solutions to the % viability_.....	39

LIST OF FIGURES

Figure 1	TNM staging and classification of Oral SCC.....	3
Figure 2	Planar structure of cisplatin.....	6
Figure 3	Graphic description of calcium polyphosphate	12
Figure 4	Cisplatin bead molds for CIP processing.....	19
Figure 5	Run 1 digital images a) Sample at 24 hours demonstrating an almost three fold increase in height. b) Sample at 48 hours, starting to slump to one side of the elution chamber. c) At 96 hours the sample continued to slump and the accumulation of viscous gel at the base of the chamber increases. d) Dried sample following 8 days of elution	26
Figure 6	Run 1 digital images of dried samples following elution for 8 days. a) Following dehydration the disks maintained their increased vertical dimension. b) The core of the sample was hollow leaving a thin shell	27
Figure 7	Digital images of G2 disks increasing in concentration of cisplatin from a control disk on the left, 50% loaded in the middle and 100% loaded to the right.....	27
Figure 8	Run 2 elution photos demonstrating exposure of the core of each disk. Note the darker core from left to right: control; 50% loaded and ; 100% loaded.....	28
Figure 9	a) Run 1 elution study, 0 to 196 hours. Cumulative release of platinum as compared to predicted load. b) Run 1, cumulative release of platinum from 0-8 hours including end point of study	30
Figure 10	a) Run 2 elution, cumulative release of platinum as represented by percent released compared to predicted loading. b) Run 2, cumulative release of platinum over the first 8 hours of elution including end point	31
Figure 11	a) Run 3 elution; Cumulative release data as represented by % of predicted cisplatin released over time. b) Run 3 elution; Cumulative release data for 0-8 hours plus endpoint data	33
Figure 12	Digital images of the miniaturized elution with two cisplatin-loaded pellets. From left to right: 30 minutes; at 2 hrs; at 192 hrs.....	34

Figure 13	a) Miniaturized elution with cisplatin-loaded pellets; cumulative release of cisplatin from 0-192 hours. b) Cumulative release of cisplatin from the G2 pellets from 0-8 hours with end point included.....	35
Figure 14	a) Combined elution data; Runs 1-3 plus miniaturized cisplatin pellet elution. b) Combined elution data for trials 1-3 plus miniaturized cisplatin pellet elution from 0-8 hours including end point.....	36
Figure 15	Digital image of a G2 axial pressed disk and a G2 CIP processed pellet	38
Figure 16	MTT assay comparing test solutions with control curve developed with fresh cisplatin solutions	40
Figure 17	One-way ANOVA plot demonstrating the differences test and control groups in the MTT assay against L1210 cells	40

ABSTRACT

Cisplatin is an effective chemotherapeutic agent for head and neck squamous cell carcinoma particularly in conjunction with radiation therapy. Unfortunately, its cytotoxic profile and associated systemic side effects limit its clinical efficacy. A localized delivery system was developed for cisplatin by processing calcium polyphosphate (CPP) in a multistep gelling protocol, with the goal of limiting its systemic toxicity and enhancing its overall clinical applicability. In addition, a novel method for processing the material was examined utilizing cold isostatic pressure (CIP) to allow for miniaturization of the system into an implantable device. The integration of cisplatin into the matrix was examined for efficient and dose dependent loading via dissolution of the final product and measurement of platinum concentrations by inductively coupled plasma optical emission spectrometry (ICP-OES). Drug release was measured *in vitro* by placing the CPP-cisplatin matrix into TRIS buffer solution while measuring the platinum concentration at given intervals from 0.5 hours to 14 days. The cytotoxicity of the cisplatin against L1210 cells was examined using an MTT assay following a 12-hour elution. The material demonstrated a predictable and dose dependent loading of cisplatin, although the release of the drug showed variability exemplified by a more pronounced burst release with aging of the stock CPP glass particulate. The CPP/cisplatin matrix exhibited cytotoxic effects after processing. This work suggests that further evaluation of this material as a matrix for cisplatin delivery should be undertaken in an attempt to normalize release, maximize the concentration within the system and further optimize the bead format in order to improve the potential for clinical usage.

LIST OF ABBREVIATIONS USED

SCC	Squamous cell carcinoma
HPV	Human papiloma virus
HNSCC	Head and neck squamous cell carcinoma
CDDP	cis-diamminedichloroplatinum (cisplatin)
HA	Hydroxyapatite
CPP	Calcium polyphosphates
CaP	Calcium phosphate
d-H ₂ O	De-ionized water
CIP	Cold isostatic pressure
PVS	Polyvinyl siloxane
ICP-OES	Inductively coupled plasma optical emission spectrometry
DMEM	Dulbecco's modified Eagle's medium

ACKNOWLEDGEMENTS

I would like to thank my supervisor, Dr Mark Filiaggi, for dedicating so much of his time in helping me with this work. I will always be thankful for your encouragement and understanding. To Maxine and Gordie for allowing me to utilize their labs and help guide me through my experiments. Trish and Arash, thank you for all of your help in the lab and putting up with my complete lack of lab experience; you were always willing to lend a hand and it made all the difference. Thank you to Martha for all of your help with my data analysis. Thank you to my thesis committee for your time and guidance in preparing this work.

To my dedicated wife and girls, for giving up so much of our time together over the last 6 years and always making even the darkest days seem bright. It was with my family's support that I was able to keep pressing on, even when it seemed like I had mountains to climb. I will work my entire life to show my appreciation for everything that you have given me.

Finally, thank you to my parents for their unwavering support over the last 37 years. I know you will always have my back.

CHAPTER 1 INTRODUCTION

1.1 HEAD AND NECK SQUAMOUS CELL CARCINOMA

Oral cancer is the sixth most common cancer worldwide. Squamous cell carcinoma (SCC) is a malignant tumor of the squamous epithelium. SCC of the head and neck accounts for approximately 5% of newly diagnosed cancers and accounts for over 500,000 new cases (1) and over 350,000 cancer deaths worldwide each year (2).

Tobacco, alcohol consumption, and more recently discovered, human papilloma virus (HPV) remain the most dominant etiologic factors implicated in oral cancer (3). Surgery is the most well established modality of initial treatment for the majority of oral cancers (4). The factors that affect treatment methods are typically related to both the tumor, the systemic health of the patient, and the wishes of the patient and their support system (5). Primary site location, tumor size, proximity to bone and vital structures, depth of infiltration, presence or absence of nodal involvement, and metastatic disease are factors which influence a particular surgical approach (5). For example, tumors that approximate or involve the mandible require specific understanding of the mechanism of bone involvement and will influence the extent of surgical resection required (6).

Due to an improved understanding of the biology of local progression, there has been a corresponding improvement in the overall survival of patients with stage I and stage II oral carcinoma over the course of the past thirty years (7). This is largely due to the early identification and treatment of metastatic lymph nodes in the neck, and employment of adjuvant post-operative radiotherapy or chemoradiotherapy (3). The role of surgery in

primary squamous cell carcinomas in other sites of the head and neck has evolved with integration of multidisciplinary treatment approaches employing chemotherapy and radiotherapy either sequentially or concurrently (8). For example, larynx preservation with concurrent chemoradiotherapy has become the standard of care for locally advanced carcinomas of the larynx or pharynx previously requiring total laryngectomy (9, 10). It is logical that as our understanding of the disease process, progression and cellular biology of oral SCC improves, more conservative surgical techniques will be employed and adjunctive treatment will play a more prominent roll.

1.1.1 Stage I, II – Surgical Treatment

T1 tumors describe a tumor that is not greater than 2cm in its greatest diameter. A T2 tumor exceeds this diameter but is not larger than 4 cm. Surgery remains the mainstay of management for a majority of T1 and T2 neoplasms arising in the head and neck area, achieving a high control rate with good functional preservation and a 5-year overall survival rate of 80-90% (11, 12). Stage I and Stage II Head and neck squamous cell carcinomas (HNSCC) involve T1 and T2 tumors with no local or distant metastasis (Figure 1).

1.1.2 Stage III, IV – Multi-modal therapy

T3 tumors are greater than 4 cm in diameter. T4 tumors are classified based on their invasion of local vital structures. T4a tumors are described as moderately advanced local disease, while T4b tumors represent very advanced local disease, with invasion of adjacent space such as the pterygoid plates or skull base, or encapsulation of the internal

carotid artery. Stage III and IV HNSCC consist of either T1 and T2 tumors with local or distant metastases, or T3 and T4 tumors with or without metastases (Figure 1).

Primary tumor (T)			
TX	Primary tumor cannot be assessed		
T0	No evidence of primary tumor		
Tis	Carcinoma in situ		
T1	Tumor ≤ 2 cm in greatest dimension		
T2	Tumor > 2 cm but ≤ 4 cm in greatest dimension		
T3	Tumor > 4 cm in greatest dimension		
T4	(lip) Tumor invades through cortical bone, inferior alveolar nerve, floor of mouth, or skin of face, ie, chin or nose ^a		
T4a	Moderately advanced local disease ^a (lip) Tumor invades through the cortical bone, mouth, or skin of the face (ie, chin or nose) (oral cavity) Tumor invades adjacent structures (eg, through cortical bone [mandible or maxilla] into the deep [extrinsic] muscle of the tongue [genioglossus, hyoglossus, palatoglossus, and styloglossus], maxillary sinus, or skin of the face)		
T4b	Very advanced local disease Tumor involves masticator space, pterygoid plates, or skull base and/or encases internal carotid artery		
Regional lymph nodes (N)			
NX	Regional nodes cannot be assessed		
N0	No regional lymph node metastasis		
N1	Metastasis in a single ipsilateral lymph node, ≤ 3 cm in greatest dimension		
N2	Metastasis in a single ipsilateral lymph node, > 3 cm ≤ 6 cm in greatest dimension; or in multiple ipsilateral lymph nodes, none > 6 cm in greatest dimension; or in bilateral or contralateral lymph nodes, none > 6 cm in greatest dimension		
N2a	Metastasis in a single ipsilateral lymph node, > 3 cm but ≤ 6 cm in greatest dimension		
N2b	Metastasis in multiple ipsilateral lymph nodes, none > 6 cm in greatest dimension		
N2c	Metastasis in bilateral or contralateral lymph nodes, none > 6 cm in greatest dimension		
N3	Metastasis in a lymph node, > 6 cm in greatest dimension		
^a Superficial erosion alone of bone/tooth socket by gingival primary is not sufficient to classify a tumor as T4.			
Distant metastases (M)			
M0	No distant metastasis		
M1	Distant metastasis		
Stage grouping			
Stage 0	Tis	N0	M0
Stage I	T1	N0	M0
Stage II	T2	N0	M0
Stage III	T3	N0	M0
	T1	N1	M0
	T2	N1	M0
Stage IVA	T3	N1	M0
	T4a	N0	M0
	T4a	N1	M0
	T1	N2	M0
	T2	N2	M0
Stage IVB	T3	N2	M0
	T4a	N2	M0
	Any T	N3	M0
Stage IVC	T4b	Any N	M0
	Any T	Any N	M1

From Edge SP Byrd DR, Compton CC, et al (eds): AJCC Cancer Staging Manual, 7th ed. New York, Springer, 2010.

Figure 1: TNM classification and staging of Oral SCC

Approximately 60% of patients with head-and-neck squamous cell carcinoma (HNSCC) present with locally advanced Stage III and IV disease(13). Despite advances in the treatment of these patients, long-term disease-free survival and overall survival have shown little improvement compared to a decade ago (14). Approximately 40% to 60% of patients develop local recurrences, and 20% to 30% will be diagnosed with distant metastatic disease (5). Because locally advanced cancer is difficult to control using surgery alone, adjunctive therapy is necessary and has resulted in a renewed interest in developing more accurate, less harmful techniques (15, 16).

1.2 CHEMOTHERAPY

Chemotherapy has emerged as an integral component in the management of locally advanced HNSCC. It has been incorporated as induction or neoadjuvant chemotherapy delivered before definitive local regional treatment, concurrently with radiation as chemoradiotherapy, or as adjuvant chemotherapy after conclusion of definitive local therapy. Multimodal approaches to treatment involving chemotherapy and radiotherapy have been extensively tested (10, 16-27). A meta-analysis of 63 trials for a total of over 10,000 patients treated with various chemotherapy and radiation regimens have helped to establish the role of concomitant chemotherapy in locally advanced SCCHN (16). This analysis identified an 8% improvement in 5-year survival when chemotherapy was added to the radiation therapy treatment regimen, and a 5% improvement with cisplatin and 5-Fluorouracil induction chemotherapy. A more recent meta-analysis including more than 17,000 patients demonstrated a 6.5% absolute survival benefit for concurrent chemotherapy, with an 11% survival benefit for concurrent cisplatin (9).

In 1950, Klopp and Alford initially reported on arterial injection therapy for head and neck cancer (28). Lee, et al. first reported the use of superselective intraarterial chemotherapy, the injection of chemotherapeutic agents directly into the feeder vessels of a tumor, for head and neck cancer via the femoral artery (29). Robbins, et al. further reported on the use of rapid superselective intra-arterial infusion of supradose cisplatin once per week combined with sodium thiosulfate for systemic cisplatin neutralization (30). In the 1990s, arterial injection therapy was re-evaluated as a new treatment option for head and neck cancer (23, 30), demonstrating the potential for localized drug delivery to the tumor bed. Localized treatments with chemotherapeutic agents have been shown to minimize systemic toxicity while having comparable anti-tumor activity when compared to a systemic dose (31, 32).

The majority of chemotherapeutic drugs can be divided into alkylating agents, antimetabolites, anthracyclines, plant alkaloids, topoisomerase inhibitors, and other antitumour agents. All of these drugs affect cell division or DNA synthesis and function in some way. Recently, there has been the introduction of agents that do not directly interfere with DNA. These drugs include monoclonal antibodies and the new tyrosine kinase inhibitors that directly target a molecular abnormality in certain types of cancer such as chronic myelogenous leukemia or gastrointestinal stromal tumors (33, 34). These are examples of targeted therapies that are a major source of contemporary research.

1.3 CISPLATIN

Cisplatin (cis-diamminedichloroplatinum or CDDP) is a chemotherapeutic drug used against a wide variety of solid tumors. It has been demonstrated to be effective to some degree against ovarian, testicular, cervical, lung, head and neck and bladder cancers in adult patients (35). It is also used as part of the standard treatment regimen for many types of pediatric cancers, including neuroblastoma, osteosarcoma and hepatoblastoma (35). Cisplatin is considered one of the most effective chemotherapeutic agents for children, with a cure rate as high as 85% (36), and along with its derivatives is the most widely used anticancer agent.

Cisplatin was first discovered by Michel Peyrone in 1845 (37). It is a water-soluble planar member of the platinum coordination complex class of anticancer drugs. Cisplatin is soluble in water or saline at 1mg/mL and in diethylformamide at 24 mg/mL (38). Unlike the complex organic molecules that comprise most chemotherapeutic agents, cisplatin is a simple inorganic molecule formed by an atom of platinum surrounded by two chloride and two ammonium groups in *cis* position of a horizontal square plane (Figure 2).

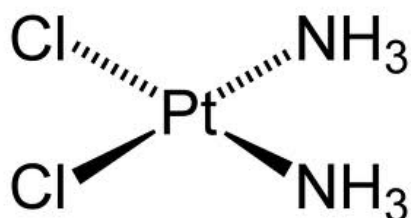


Figure 2: Planar structure of cisplatin

CDDP's anti-tumor potential was discovered in the 1960s after observations from Barnett Rosenberg's group on its capacity to inhibit bacterial fission and retard the growth of sarcomas transplanted into a mouse model (39). The earliest reported use of cisplatin on human subjects was carried out by Hill's group in 1975 (40) and demonstrated its efficacy against several human malignancies. It was first approved in North America for clinical use in humans in 1978.

Cisplatin is highly toxic for proliferating cells. It is believed that DNA is its main target, where it forms complexes with two 7-N-guanine residues within double helix DNA. These covalent bonds distort the natural structure of the double helix and impede its replication by preventing uncoiling during mitosis (35). Cisplatin and its derivatives carboplatin, oxilaplatin and other platinum analogues are considered alkylating agents or, more accurately alkylating-like agents, as they do not contain an alkyl group. The alkylating agent class of chemotherapeutics has the ability to alkylate many nucleophilic functional groups under the conditions present within a cell. They impair cell function by forming covalent bonds with the amino, carboxyl, sulfhydryl, and phosphate groups in biologically important molecules. By directly interacting with intracellular molecules including proteins, DNA and lipids, cisplatin disrupts multiple essential cellular structures and organelles, ultimately inhibiting cell function and activating apoptosis of the affected cells (41).

The therapeutic effect of cisplatin is based on its cytotoxicity; however, cytotoxicity is also the cause of the side effects that limit its clinical usage (38, 41). In this regard,

CDDP functions in a non-selective manner and will interact with non-cancerous cells and proteins. Side effects occur more frequently at higher dosages by acting on non-proliferating cell types that are less susceptible at lower dosages (35). The kidneys, liver, prostate, spleen, bladder, muscle, testicles, pancreas, bowel, adrenal glands, heart, lung, cerebrum and cerebellum tend to accumulate the drug (38). The most commonly reported systemic side effects are nephrotoxicity via tubular necrosis, ototoxicity via cochlear damage, and peripheral sensory neuropathy. Renal toxicity is the most serious complication, restricting the dosage and clinical use and subsequently the anticancer efficacy of cisplatin.

Due to the significant systemic toxicity and subsequent side effects of CDDP, a second generation of compounds was developed in an attempt to alleviate some of these effects. Carboplatin and Oxaliplatin are the two most commonly used of the second generation drugs and do show an improved systemic toxic profile; however, they have failed to fully address all of the problems with CDDP. When compared to cisplatin for the treatment of head and neck cancers, carboplatin has been shown to have a decreased tumor response for adjuvant chemoradiotherapy (42).

The primary role of cisplatin in HNSCC is that of a radiosensitizing agent (43, 44). A radiosensitizer is an agent that increases the effectiveness of radiation therapy, thereby enhancing tumor response (45). There are numerous reports on the advantages of concurrent cisplatin and radiotherapy treatments for the treatment of HNSCC (9, 46-51). The current recommendations by the Radiation Therapy Oncology Group (United States)

and the European Organization Research and Treatment of Cancer recommend the addition of relatively high doses of cisplatin on days 1, 22 and 43 of post-operative radiotherapy based on Phase 3 studies. As with all cisplatin treatment protocols, the balance between therapeutic effects and systemic toxicity of cisplatin based chemoradiation can hinder optimal dosing regimens (52, 53). Selective intra-arterial administration of cisplatin to oral SCC has demonstrated the benefits of continuous low-dose administration of cisplatin when used throughout the radiation therapy cycle (10, 54). The ideal local delivery system for cisplatin would have a release profile that mimics this continuous dosing of cisplatin to the tumor bed, maintaining therapeutic levels of the drug at the target tissue while limiting whole body dosing.

1.4 CISPLATIN AND SUSTAINED RELEASE COMPOUNDS

One of the challenges with current cancer treatments is how to deliver drugs to tumors without causing debilitating side effects. Whole-body dosing can also lead to systemic toxicity. The usual protocol to deliver CDDP is by parenteral administration, creating a high initial intravascular dose that is rapidly distributed to the entire body. By delivering drugs in a more targeted or local manner, some of the side effects can be reduced (55). Implantable drug delivery systems can achieve high local concentrations of a drug while maintaining lower serum concentrations. These delivery systems are an emerging area of study designed to provide alternative methods of treatment to clinicians and patients. In compromised wound sites, avascular regions can inhibit the delivery of a drug to the targeted tissue; localized delivery also remedies this by allowing drugs to reach their target tissue by diffusion (31, 56).

The ability to locally deliver cisplatin directly to the tumor bed may improve the pharmaco-toxicological profile of this drug by locally exploiting its cytotoxicity while keeping its systemic side effects to a minimum. Several materials have been investigated as carriers for CDDP, with the majority being calcium phosphates (CaP) due to their biocompatibility (55, 57-59). A significant volume of work has focused on incorporating solid state CDDP with hydroxyapatite (HA) ceramic or solid phase cement (55, 58, 59). The tissue distribution of CDDP from these implanted systems depended on a series of events involving dissolution of the drug, adsorption of the drug to the CaP and concentration gradients within the host tissue (60). In animal models, these loaded matrices provided tumor inhibition with a significantly lower and less toxic systemic dose when implanted adjacent to tumors (55, 58, 61). More contemporary work has focused on adsorption of agents onto the crystalline form of CaP rather than the incorporation of solid-state drugs. Using these methods, the delivery of chemotherapeutic agents (57, 58) as well as steroids (62), hormones (63) and proteins (64) have been demonstrated using HA and tricalcium phosphate ceramics. The adsorption and release of CDDP from HA crystals has been shown to be dependent on the crystallinity of the HA as well as the temperature and chloride concentration of the medium (60, 65).

Nanotechnology-based materials processing has developed rapidly in recent years, and there have been several attempts at incorporating CDDP into these systems (66-68). Swet, et al. evaluated a silica-calcium-phosphate nanocomposite as a CDDP drug delivery system and found improved tumor response *in vivo* with a hepatocellular model carcinoma when compared to conventional intravenous cisplatin treatment, without any

of the associated systemic side effects observed (68). Fan, et al. developed a rattle-structured nanocapsule to deliver CDDP directly to tumors for radiosensitization and demonstrated similar results, with improved treatment outcomes and significantly reduced systemic side effects (67).

1.5 CALCIUM POLYPHOSPHATE

Calcium polyphosphates (CPP) are inorganic polymers have a Ca/P ratio of less than or equal to 0.5, resulting in a hygroscopic polymeric structure of linked phosphate tetrahedra cross-linked by Ca^{2+} molecules (69). CPP may exist either in a crystalline form or as an amorphous glass, with these condensed calcium phosphates generally exhibiting a linear chain structure (Figure 3).

CPP has been investigated particularly as possible bone replacement materials, as it is considered biocompatible and osteoconductive; in its crystalline form, CPP degrades to a non-toxic salt, calcium orthophosphate, which is further metabolized by the body (69).

The biocompatibility of CPP was first demonstrated in 1977 following implantation of CPP rods into rat femurs (70).

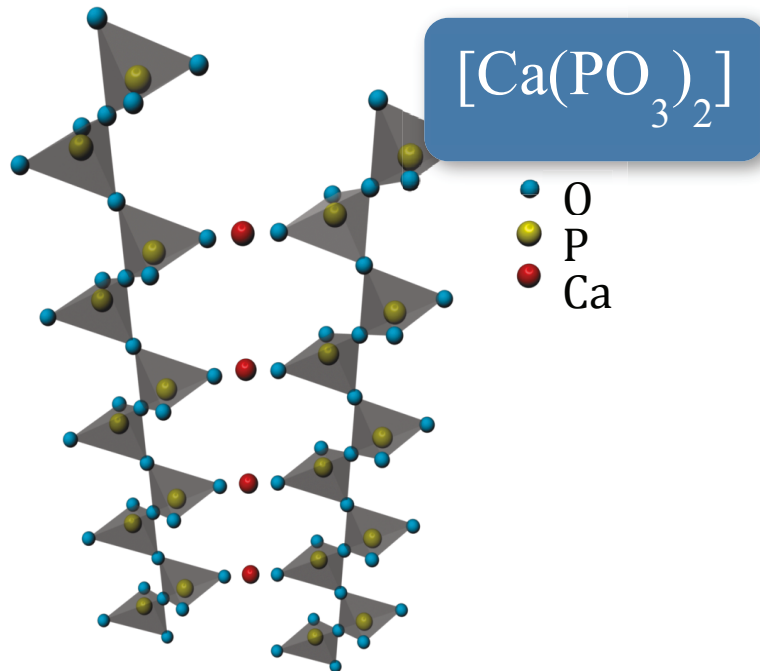


Figure 3: Graphic description of calcium polyphosphate.

Several studies have demonstrated the potential viability of amorphous long chain calcium polyphosphate as a carrier matrix in a local drug delivery system for antibiotics (71-74). In 2008 Kim et al. demonstrated the potential of the system to deliver methotrexate, an anti-cancer drug (75). These systems incorporate the drug in a gelling protocol that exposes amorphous calcium polyphosphate to high humidity followed by drying, creating a “G1” disk (73). Particulate generated from the drug-loaded G1 disk is subsequently subjected to a compaction and regelling protocol to produce a “G2” disk. This reprocessing enables more consistent distribution of the drug throughout the CPP matrix, essentially eliminating burst release and extending release over time on the order of weeks (74). One of the advantages of this processing method is that it can be carried out at physiological temperatures and therefore does not cause heat degradation of the incorporated drug (73). The release of the drug from the calcium polyphosphate matrix occurs through diffusion of the drug out of the matrix as well as degradation of the matrix

itself, as evidenced by liberation of the drug at a faster rate than matrix resorption (61, 74, 76).

The potential for long chain calcium polyphosphate to act as a drug delivery system for cisplatin could provide advances in clinical care of patients with susceptible tumors. As the clinical efficacy of cisplatin is frequently dictated by its systemic toxicity, limiting the effective dose, this local delivery system has the potential to increase the concentration of the drug within the tumor bed while keeping the systemic concentration within a tolerable level. In advanced head and neck squamous cell carcinoma where a multidisciplinary treatment protocol is often required, limiting the systemic side-effects of any of the treatment modalities could allow clinicians to maximize treatment effect without unnecessarily compromising the patients health.

1.6 OBJECTIVES

The global objective of this thesis was to develop a localized cisplatin delivery system utilizing a CPP matrix for the adjunctive treatment of head and neck SCC. The ultimate goal of such a system will be to maintain high, clinically relevant local concentrations of cisplatin while limiting systemic side effects. To realize this goal, the following objectives were undertaken:

Objective 1: Incorporation of Cisplatin into a CPP matrix

The loading of cisplatin into CPP will be completed according to the “gelling” protocol described by Dion et al. in previously published works (73). Earlier, preliminary studies

(unpublished) by the Filiaggi group at Dalhousie University had demonstrated the viability of incorporating cisplatin into CPP. We will further this work by determining the optimum methodology and concentration of cisplatin to be incorporated into the CPP.

Hypothesis: Cisplatin will incorporate into CPP in an efficient and dose-dependent manner.

It has been well documented that several antibiotics as well as the chemotherapeutic agent methotrexate have been readily loaded into calcium polyphosphate glass (72-75). Due to the hygroscopic nature of the CPP molecule and the water solubility of cisplatin, it is expected that uptake of the drug will occur in a predictable fashion. However, as cisplatin is an inorganic, metal containing molecule, the reliability of incorporation may be affected.

Objective 2: To determine to release characteristics of cisplatin from CPP

Following the loading of cisplatin into the CPP, the rate and duration of release from the matrix will be quantified.

Hypothesis: The release of cisplatin from CPP will occur at a steady rate and not demonstrate burst release shown by some other drug delivery systems.

As with other drugs incorporated into CPP (Vancomycin, cefuroxime and methotrexate) via the gelling process (71, 72, 74, 75), it is predicted that there will be a significant decrease in the early “burst release” of cisplatin during drug elution. It is postulated that the release of cisplatin will occur in a consistent and predictable rate from the CPP matrix.

Objective 3: To evaluate the activity of the cisplatin following incorporation and release from the CPP matrix

The cytotoxic activity of cisplatin can be evaluated *in vitro* by testing the eluted drug against known susceptible tumor cells.

Hypothesis: Cisplatin will continue to be active following incorporation into the CPP matrix.

Previous studies have demonstrated that cisplatin can be incorporated into drug delivery systems and eluted without negatively affecting the cytotoxic nature of the drug (31, 32, 60). Testing the elution media against susceptible cells and comparing the results against those of cisplatin alone and calcium polyphosphate alone can verify the viability of cisplatin activity.

Objective 4: To re-format the delivery matrix in order to improve clinical application in head and neck squamous cell carcinoma therapy

In order for this approach to be viable in a clinical setting, a smaller and reproducible delivery matrix that can be implanted into soft tissue using an existing implant trocar needs to be developed.

Hypothesis: A minitiated bead format with similar drug delivery characteristics of the larger disk format can be achieved using a cold isostatic pressing approach.

CHAPTER 2 MATERIALS AND METHODS

2.1 MATRIX PREPARATION

Established protocols for CPP production were followed (74). Condensed calcium polyphosphate powder was formed via calcination of calcium phosphate monobasic monohydrate crystals ($\text{Ca}[\text{H}_2\text{PO}_4]_2 \cdot \text{H}_2\text{O}$; Sigma-Aldrich) for 10 hours at 500°C (Thermolyne Type 46200 High Temperature Furnace) in a platinum-5% gold crucible. Following calcination, the crystals were melted at 1100°C for 2 hours to allow for polyphosphate chain growth. The melted glass was then quenched in de-ionized distilled water at room temperature, resulting in an amorphous calcium polyphosphate glass. To prevent injury, some of the tension within the newly formed glass was released by striking the particles with a mortar and pestle. Impurities and residual water were removed by washing the resultant frit three times with anhydrous ethyl alcohol and allowing drying under vacuum for 24 hours. Subsequently, the washed frit was ground via a planetary ball mill (Fritsch Planetary Micro Mill) with sintered corundum mortars and balls at 6-minute intervals. The resulting powder was run through a $45\mu\text{m}$ standard test sieve (Laboratory Test Sieves, Fisher Scientific) on an Octagon D200 sieve shaker (Endecotts) and $<45\mu\text{m}$ particles were collected. Particles greater than $45\mu\text{m}$ were returned to the planetary micro mill and ground for an additional 6 minutes. This process was repeated up to four times. All of the $<45\mu\text{m}$ powder was transferred to glass scintillation vials and stored in a desiccant chamber under vacuum.

2.2 DRUG LOADING AND G1 DISK PRODUCTION

A stock solution of cisplatin, >99.9% trace metals basis, (Sigma-Aldrich) was prepared according to manufacturer's recommendations immediately prior to processing for each experiment. De-ionized water (d-H₂O) was maintained at 37°C and 10mg of cisplatin was added to 10 mL of d-H₂O in glass scintillation vials. The solution was vortexed for 30 seconds every minute for 5 minutes. The resultant mixture was passed through 0.45µm syringe filters to remove any un-dissolved particulate. The filtered solution was analyzed via ICP-OES (PerkinElmer Inc) to confirm the desired Platinum concentration of 0.8-1 mg/mL.

G1 disks were fabricated by combining 60.2 µL of the aforementioned cisplatin solution for every 150 mg of the <45µm CPP powder (71). The G1 disks were produced in batches of 10 and thus 602 µL of cisplatin solution was mixed with 1500 mg of CPP powder. The powder was placed on a room temperature glass block and hollowed in the center where the solution was added. The liquid and powder was combined with a mixing spatula until a uniform consistency was achieved. Subsequently, the slurry was transferred into 8mm diameter x 2mm deep polyvinyl siloxane (PVS) molds and held at 37°C in a 100% humidity chamber for 5 hours. The "gelled" disks were removed from the humidity chamber and allowed to dry for a further 24 hours at 37°C in room air (71). The disks were immediately reprocessed for G2 disk fabrication (74). Control "blank" disks were fabricated in parallel by replacing the cisplatin solution with d-H₂O.

2.3 G2 DISK AND PELLET FABRICATION

G2 disks were produced by a compaction and re-gelling protocol that allows for more favorable release characteristics (74). G1 disks were ground in a Fritsh Planetary Micro Mill for 6 minute to <45 μm particles with the aid of a 45 μm test sieve. Larger particles were reprocessed up to 3 times until the majority of the powder was suitable for use. Each G2 disk was fabricated by placing 135 mg of <45 μm G1 powder into a 8mm diameter stainless steel punch die system. The die was compressed at 113MPa (2500 psi) and held for 5 minutes, conditions found to maximize work imparted to the powder allowing for granular rearrangement rather than the granular deformation that occurs at higher pressures (74). The die containing the compacted powder was placed into a sealed vessel at 37°C and 100% humidity and allowed to “re-gel” for 5 hours. Again the disks were removed from the vessel and allowed to dry in room air at 37°C for 24 hours. These G2 disks were used to carry out the elution experiments with the exception of the CIP bead elution study.

To confirm loading concentrations, samples of the respective cisplatin loaded disks were dissolved prior to the elution process. To test Hypothesis 1, cisplatin incorporation into the CPP matrix in an efficient and dose-dependent manner, 100% and 50% loaded disks were placed in 15 mL falcon tubes and submerged in 10 mL of 8M Nitric acid. The disks were held in a 100°C water bath for one hour and vortexed at 15 minute intervals. Following complete dissolution of the disks the resultant solution was diluted 10 fold (1 mL of solution in 9 mL of d-H₂O) and analyzed via ICP-OES to confirm cisplatin loading.

To improve the clinical application for HNSCC (Hypothesis 4), cold isostatic pressure (CIP) was used to create 2mm diameter beads of CPP with and without cisplatin. CIP is a process whereby hydraulic pressure is used to impart multi-axial pressure on ceramic samples to create greater uniformity of compaction and homogeneity compared to conventional uniaxial pressing. It is based on the principle espoused by French scientist Blaise Pascal, Pascal's law: "A change in the pressure of an enclosed incompressible fluid is conveyed undiminished to every part of the fluid and to the surface of its container" (77). Powder materials are placed into molds that have a low resistance to deformation and sealed in airtight packages. Compression is then applied uniformly by transmitting the fluid pressure. CIP Molds were fabricated by imbedding evenly spaced 2 mm ball bearings into polyvinyl siloxane (PVS). The molds were 3mm in thickness with the ball bearings directly abutting one side of the mold to allow for filling with the CPP powder, and 1mm of thickness on the other side (Figure 4).

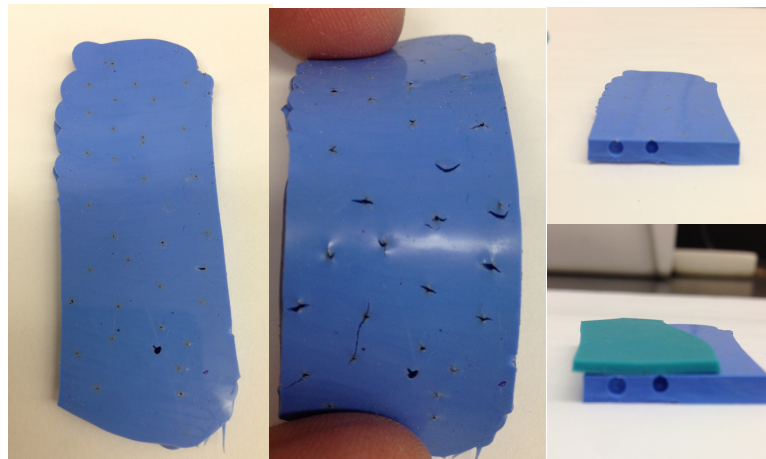


Figure 4: Cisplatin bead molds for CIP processing

Following sufficient time for curing, the ball bearings were removed from the thin side of the PVS and $<45\mu\text{m}$ G1 CPP powder was packed into each of the spherical voids. A 1mm sheet of PVS was placed over the PVS mold where the bearings abutted the side to allow for equal material surrounding the powder (Figure 4). Each of the molds was vacuum-sealed in vinyl bags for CIP processing. Both cisplatin loaded and control blank powder was used for processing. Within the cold isostatic press (Ilishin Auto Clave Co., Ltd.) a consistent 3000 kPa pressure was applied to the molds for 5 minutes to maximize work imparted on the material. The CIP compacted spheres were removed from the molds and placed into a 100% humidity chamber at 37°C for one hour to allow for G2 gelling.

2.4 ELUTION PROTOCOL

Cisplatin release from the G2 disks was quantified by placing the prepared disks into cornea viewing chambers along with 15 mL of 0.1M Tris-buffered saline (pH 7.6). The Tris buffer solution was prepared by dissolving 3.32 g Tris Base, 11.44 g Tris-HCl and 8.77 g NaCl (Sigma-Aldrich Co. LLC) in 1 L of d- H_2O . All components were combined in a 1.5 L flask with a magnetic stirrer until dissolved. 6M HCl was added dropwise until a final pH of 7.6 was achieved. The chambers were gently agitated at 90 rpm on a digital orbital mixer (VWR International LLC) in a 37°C chamber. Platinum concentration of the eluted media was analyzed by removing 7mL samples of the buffered elution medium from the viewing chambers at predetermined time intervals. Samples were taken at 30 min, 1 hr, 2 hr, 4 hr, 8 hr, 24 hr, 48 hr, 96 hr and 192 hrs. The 7 mL of elution medium was replaced with 7 mL of fresh 0.1 M Tris-buffered saline. In order to correct for

volume losses due to evaporation, the mass of the chambers before and after media removal and replenishment was recorded and additional media was added to maintain consistent volume.

Following completion of the elution experiments the remaining samples were dissolved in 10 mL of 8M Nitric acid at 100°C for 1 hour to release any remaining cisplatin and confirm the original cisplatin load. Cisplatin concentrations were reported as cumulative release by mass as well as the % release rate based on the experimentally determined loading efficiency of the available cisplatin into the G2 disk. Each treatment group had an n=7, with controls in triplicate (n=3). The elution experiments were repeated three times using the same experimental protocols, and are referred to as run 1, run 2 and run 3.

2.5 CISPLATIN RELEASE MEASUREMENTS

Cisplatin concentrations were determined within the elution medium by measuring the levels of platinum present. Each of the 7mL samples was filtered through 0.45 µm syringe filters to remove particulate matter. Platinum was measured at the predetermined intervals by ICP-OES (74). In an attempt to maximize accuracy of the analysis, platinum standards were used that bracketed elution concentrations.

2.6 MINIATURIZED ELUTION

A modified elution protocol was developed to compensate for the reduced size of the specimen. Rather than use a horizontal orbital shaker, 2mL round bottomed Eppendorf tubes were placed into a vertical rotating mixer (Appropriate Technical Resources).

1.5mL of Tris Buffer solution and two of the 2mm beads were added to each tube. There were seven cisplatin-loaded groups and three control blank groups. The mixer was placed into a 37°C chamber, angulated at 45° from horizontal to minimize abrupt impact on the beads while rotating vertically and set at a constant 8rpm. At the predetermined intervals of 30 minutes, 1, 2, 4, 8, 24, 48, 96, and 192 hours, 0.7mL of elution media was removed and replaced with an equivalent volume of fresh Tris buffer solution. The removed elution samples were filtered through 0.45µm syringe filters and 0.5 mL was added to 4.5mL de-ionized H₂O and subsequently analyzed for platinum content by ICP-OES. To determine the remaining platinum concentration following completion of the elution study, the remaining CIP compressed beads were dissolved for one hour at 100°C in 1 mL of 8M Nitric acid. 0.5mL of the resultant solution was added to 4.5 mL of de-ionized water and analyzed by ICP-OES.

A simple apparent density measurement for the CIP manufactured spheres was determined measuring their diameter (to calculate volume) and weight. This was compared to the apparent density obtained with the G2 disks.

2.7 CISPLATIN VIABILITY

Murine L-1210 acute lymphoblastic leukemia cells (ATCC, Manassas, USA) were used to evaluate cisplatin action after processing into G2 CPP disks(78-82). As per vendor instructions, the cells were suspended in Dulbecco's modified Eagle's medium (DMEM) (ATCC, Manassas, USA) supplemented with horse serum (ATCC, Manassas, USA) to a final concentration of 10% and incubated at 37°C in a 5% CO₂ environment within plastic

culture flasks. Cultures were maintained by removal and replacement of 30% by volume of fresh media every two days.

G2 CPP-cisplatin (loaded) disks and CPP (unloaded) disks were fabricated as described previously. Three disks were added to each corneal viewing chamber in 15mL of DMEM with 10% horse serum and eluted at 37°C on a horizontal oscillating table at 100RPM. 10mL of elution media was removed from each flask at 12 hours and passed through 0.45µm syringe filters. The platinum concentrations of the filtered solutions were evaluated via ICP-OES and cisplatin concentrations were extrapolated by multiplying by the platinum concentration by 1/65.016 as cisplatin is 65.016% platinum by weight). Two additional unloaded G2 controls were run in parallel.

Cell viability was assessed using a standard MTT (3-(4,5-dimethylthiazol-2-yl)-5-diphenyltetrazolium bromide assay (Sigma Chemical Co). L1210 cells were collected and dispensed to 96-well, round bottomed micro plates at a concentration of 4×10^5 cells in 50µL of growth medium as determined with a hemocytometer. Cell viability was confirmed by treating the cells with Trypan Blue staining prior to counting. The cells were then treated with 50µL of the filtered elution solutions at full and 50% concentrations. Positive controls were achieved by adding 50µL of stock cisplatin solutions with platinum concentrations of 20ppm, 15ppm, 10ppm and 5ppm in DMEM and 10% horse serum for final concentrations of 10ppm, 7.5ppm, 5ppm and 2.5ppm respectively. DMEM and 5% horse serum only acted as the negative control. Each of the treated and control groups was tested in three parallel wells. Following 24 hours of

incubation at 37°C in 5% CO₂, 10µL of 5 mg/mL MTT was added to each well and incubated for an additional 4 hours. The plate was then centrifuged at 1400rpm for 5 minutes. The supernatant was removed and 100µL of DMSO was added to each well for cell lysis and dissolution of the formazan crystals. Control blanks were carried out by adding 50µL of DMSO to incubated wells at T₀. The plates were read on an automated microplate spectrophotometer at 570 nm for optical density (OD).

Cell viability was carried out using the following formula:

$$\text{Cell viability \%} = \frac{(\text{OD}_T - \text{OD}_B)}{(\text{OD}_N - \text{OD}_B)} \times 100$$

where OD_T, OD_B, and OD_N are the optical densities of the treated, blank and negative control wells respectively.

2.8 STATISTICAL ANALYSIS

All statistics were calculated using SPSS software for windows. Incorporation of cisplatin in a dose dependent manner and density comparisons between CIP and axial preeede samples were examined using independent samples t-test. Levene's test for equality of variances was used to examine the variability of the MTT assay groups. One-way analysis of variance (ANOVA) and independent samples t-test were used to compare groups within the MTT assay. All tests were examined using a significance level of p=0.05.

CHAPTER 3 RESULTS

3.1 DOSE DEPENDENT LOADING STUDY

The 100% stock solution contained 684.5ppm(mg/L) Pt and the 50% solution contained 335.9ppm(mg/L) Pt. Based on the solution concentrations the predicted loading of Pt per mg of G1 material was 0.135ug for the 50% material and 0.274ug for the 100% material. The measured loading of the 50% material was 0.1017ug Pt/mg, or 75% of the predicted load, while the measured load of the 100% material was 0.1942ug Pt/mg, or 71% of predicted load, confirming Hypothesis 1 (efficient and dose dependent loading of cisplatin within the CPP system); there was no significant difference in the loading efficiency between 100% and 50% groups ($p=0.164$). The ratio of incorporated cisplatin for the 50% loaded disk to the 100% loaded disk was 0.52:1.

Table 1: Dose dependent loading of a fully saturated cisplatin solution vs. the saturated solution diluted by 50%

Material	Mass (mg)	PPM (measured)	mg Pt / disk	mg Pt/mg disk	% Predicted
50% 1	100.5	0.099	0.0099	0.0000985	72.96
50% 2	145.7	0.145	0.0145	0.0000995	73.70
50% 3	159.9	0.171	0.0171	0.000107	79.26
100% 1	107.2	0.214	0.0214	0.0001996	72.66
100% 2	141.8	0.261	0.0261	0.0001841	67.02
100% 3	151.3	0.301	0.0301	0.0001989	72.41

3.2 ELUTION STUDY

During processing of the G2 disks it was observed that the cisplatin-loaded disks were darker than the unloaded disks. Some degree of swelling was observed for all disks in the elution runs, consistent with previous observations for this matrix (73); however, the extent of swelling did vary from run to run. Run 1 demonstrated the greatest expansion of

the disks. Here, samples had a nominal increase in height within the first 4 hours and by 8 hours had approximately doubled in height (Figure 5). There was an accumulation of a viscous gel around the base of the samples as they continued to expand, and by 24 hours they had increased to about three times their original height while only increasing slightly in diameter. By 48 hours the disks had slumped slightly and continued to collapse until day 8 while increasing in diameter. The control samples behaved in a similar manner to the loaded disks; however, the degree of vertical expansion was not as great, expanding to only approximately two times its original dimension.

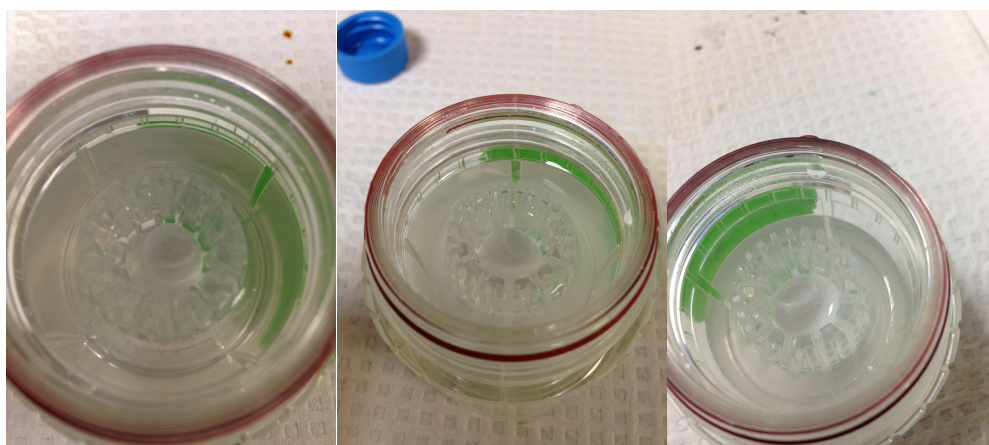


Figure 5: Run 1 digital images a) Sample at 24 hours demonstrating an almost three fold increase in height. b) Sample at 48 hours, starting to slump to one side of the elution chamber. c) At 96 hours the sample continued to slump and the accumulation of viscous gel at the base of the chamber increases.

Following elution the samples were dried and maintained their post elution dimensions (Figure 6); each was composed of a thin outer shell with a hollowed core, presumably the source of the viscous gel lining the bottom of the viewing chamber. These observations were consistent with those noted previously for vancomycin-loaded CPP disks (71).

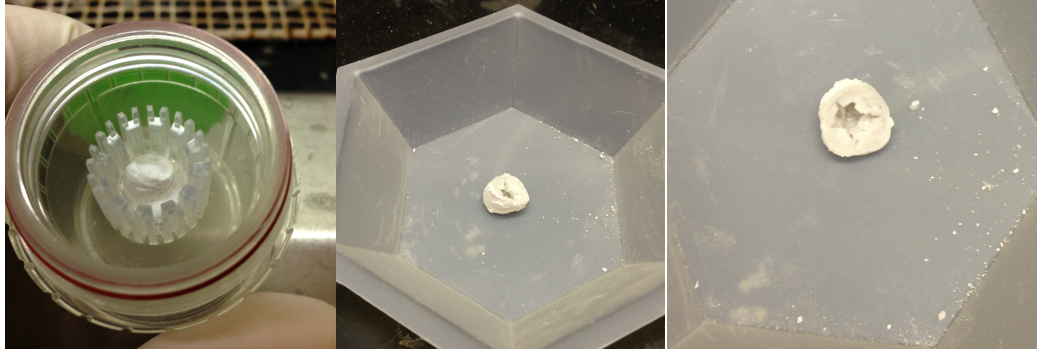


Figure 6: Run 1 digital images of dried samples following elution for 8 days. a) Dried sample following 8 days of elution. b) Following dehydration the disks maintained their increased vertical dimension. c) The core of the sample was hollow, leaving a thin shell.

Runs 2 and 3 were completed with both saturated and 50% loaded disks. It was observed following the gelling of the G2 disks that there was a darkening of the disks with an increase in the concentration of cisplatin (Figure 7).



Figure 7: Digital images of G2 disks increasing in concentration of cisplatin from a control disk on the left, 50% loaded in the middle and 100% loaded to the right.

For Runs 2 and 3, disk expansion was not as predictable or as pronounced relative to the observations made for Run 1. Run 2 disks initially expanded by about 50% in both height and width at 4 hours (Figure 8); by 8 hours the surface layer of the disks had fractured from the body of the disk exposing the inner core, and by 24 hours the fractured portion of the disk had fallen back to the body of the disk, remaining attached for the duration of the elution study. The disks continued to expand in the horizontal plane with

little change in vertical height. For Run 3, disks underwent an initial expansion in the vertical and horizontal planes, again swelling by approximately 50% within the first 4 hours; however, they slumped rapidly filling the bottom of the elution chamber, and remained unchanged in appearance for the remainder of the elution. Control samples behaved similarly to their loaded counterparts in each of these trials.

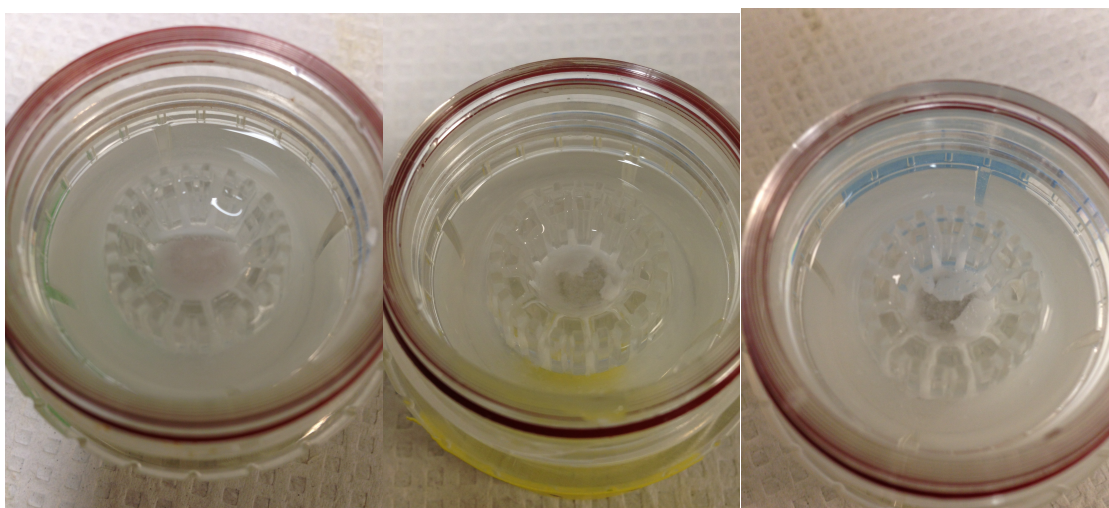


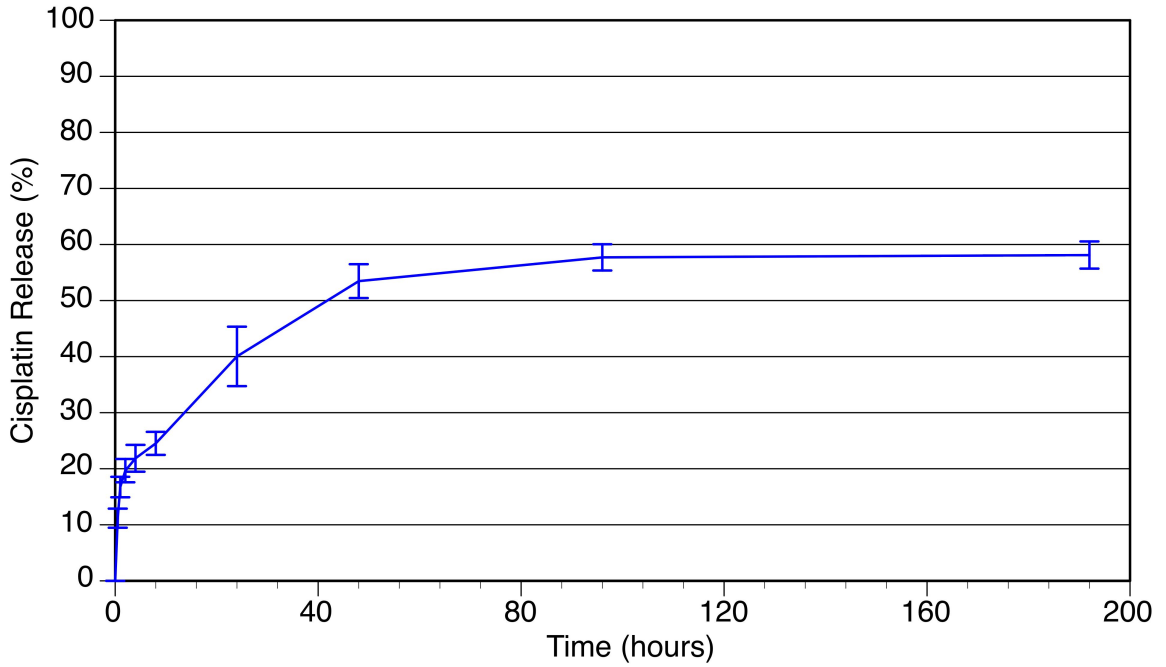
Figure 8: Run 2 elution photos demonstrating exposure of the core of each disk. Note the darker core from left to right: control; ; 50% loaded and ; 100% loaded.

3.3 CISPLATIN RELEASE

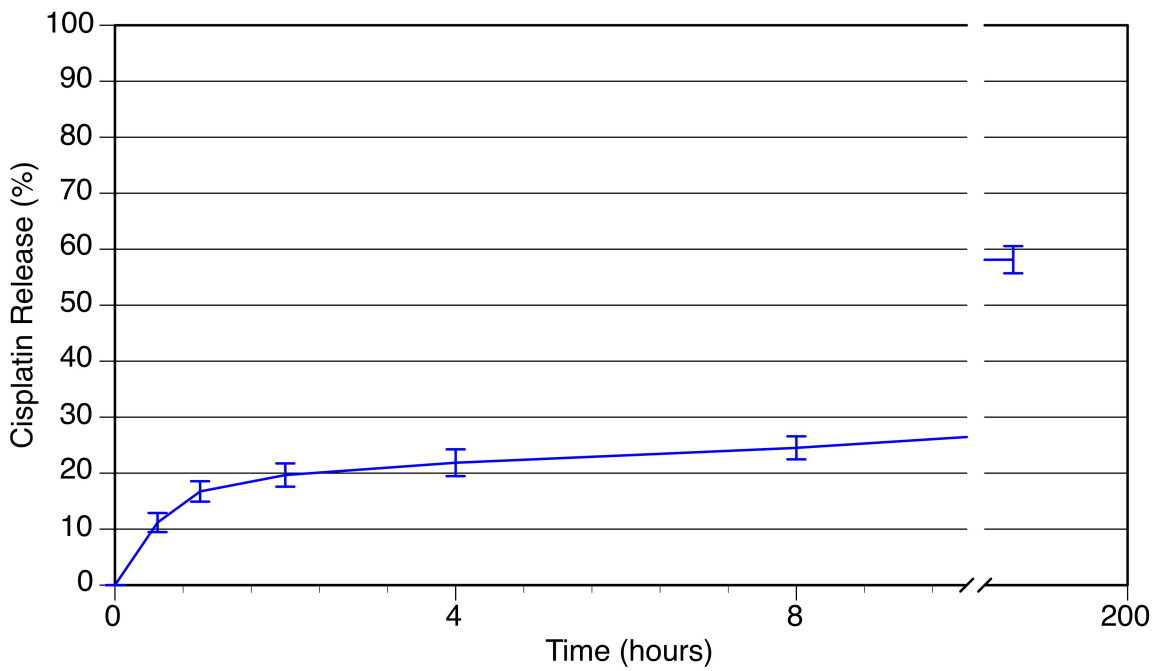
Hypothesis 2 (cisplatin release from CPP will occur at a steady rate and not demonstrate burst release) was examined in the three elution runs and the cisplatin bead elution.

Cumulative cisplatin release based on Platinum levels is described for Runs 1, 2 and 3 in Figures 9, 10 and 11, respectively, with a graphical compilation of all release data provided in Figure 14. Each of the runs demonstrated an initial burst release of platinum for the first 4 hours, followed by a slower rate of release until a plateau was reached. Run 1, completed with 100% loaded disks only, demonstrated the most consistent release profile, with a more muted burst release within the first 4 hours compared to that

observed in runs 2 and 3 (Figure 14b). This initial release was followed by a leveling off of release from 4 to 48 hours. Subsequently, release continued for the next 48 hours, with a plateau effectively reached at 96 hours through to the completion of the study. The predicted concentration of platinum in each disk was calculated by dissolving G2 disks fabricated in parallel with the elution samples. Run 1 G2 disks were predicted to contain 0.229 μ g/mg of platinum, and this was used to predict the total concentration contained in each disk. Following completion of the elution study, the remaining disk and any material within the chamber was dehydrated, dissolved, measured and added to the total eluted Pt to calculate the total cisplatin recovered based on initial loading. After 196 hours of elution, 58.12% of the predicted Pt was released from the G2 disks and 76.76% \pm 3.63 of the predicted platinum was recovered following dissolution, with 23% remaining unaccounted for. The methodology for platinum recapture was adjusted for runs 2 and 3 resulting in improved recovery of residual platinum from the dried matrix and elution chamber. The alteration in methodology included collecting the entire contents of the elution vessel, followed by rinsing the walls of the elution chamber into a 50 mL falcon tube. This allowed for recovery of platinum that would have previously been adhered to the walls and base of the chamber after being dehydrated.



(a)



(b)

Figure 9: a) Run 1 elution study from 0 to 196 hours. Cumulative release of platinum as compared to predicted load. b) Run 1, cumulative release of platinum from 0-8 hours, including end point of study.

Run 2 demonstrated a more pronounced burst release of Pt for both 50% and 100% loaded disks compared to run 1, and reached plateau by 8 hours, earlier than in the previous elution (Figure 14a). For run 2 the concentration of Pt within the 100% and 50% loaded disks was predicted to be $0.194\mu\text{g}/\text{mg}$ and $0.101\mu\text{g}/\text{ml}$, respectively. At the completion of 384 hours of eluting time, $50.67\% \pm 0.93$ of the total platinum was released from the 100% disks and 51.87 ± 2.27 was released from the 50% disks. The total cisplatin recovered following elution and dissolution of the remaining G2 material was $86.39\% \pm 1.06$ and $84.08\% \pm 3.83$ for the 100% and 50% loaded disks, respectively. Throughout the entire elution the 50% and 100% cumulative release curves overlapped, suggesting a consistent dose dependent release.

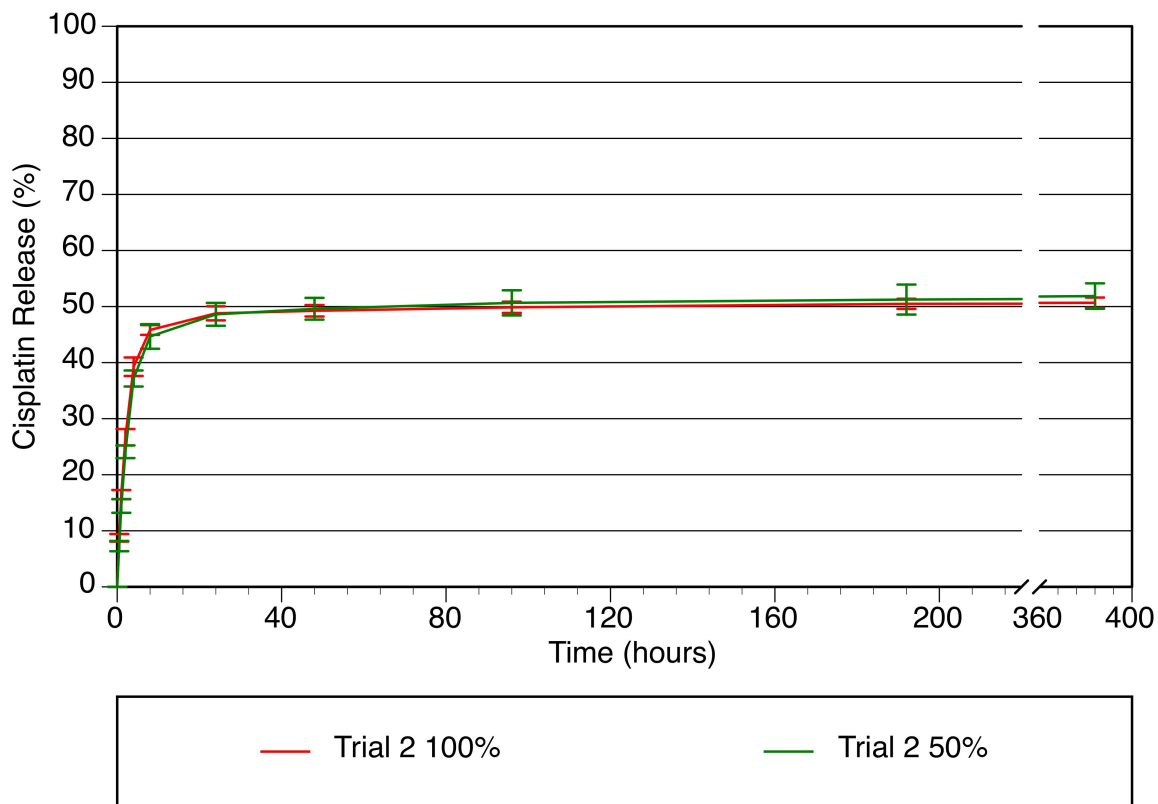


Figure 10a: Run 2 elution, cumulative release of platinum as represented by percent released compared to predicted loading.

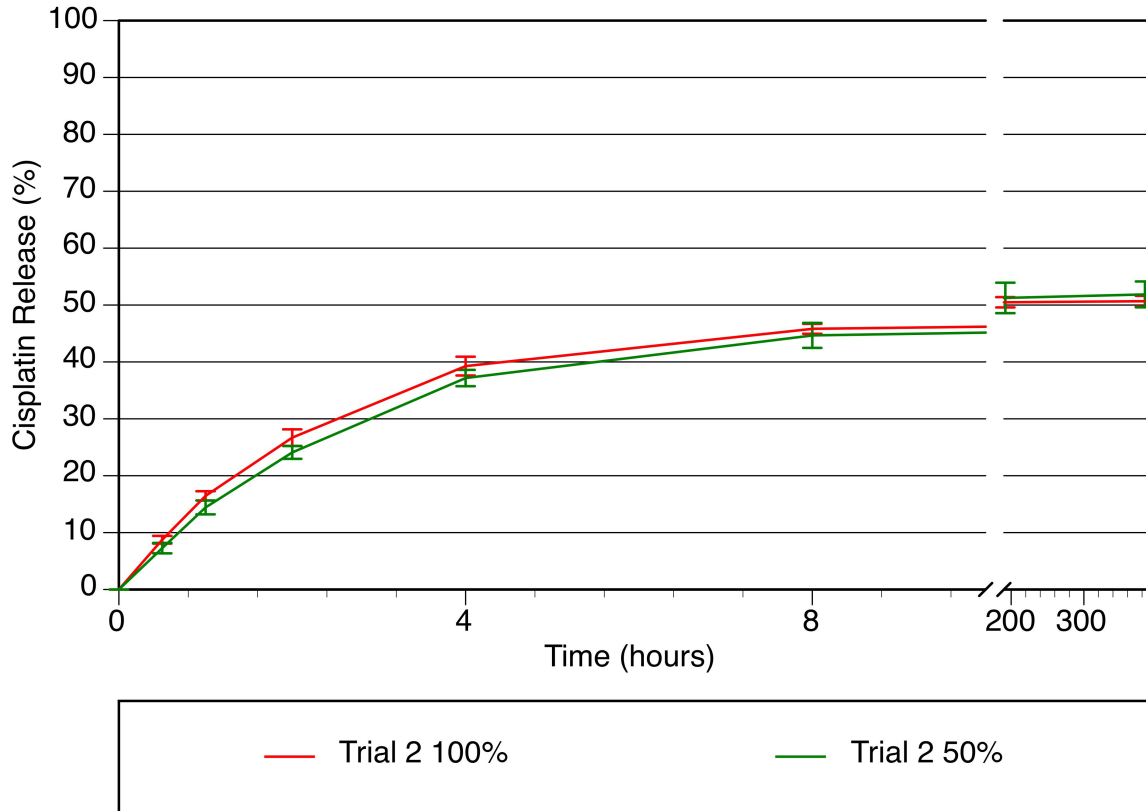
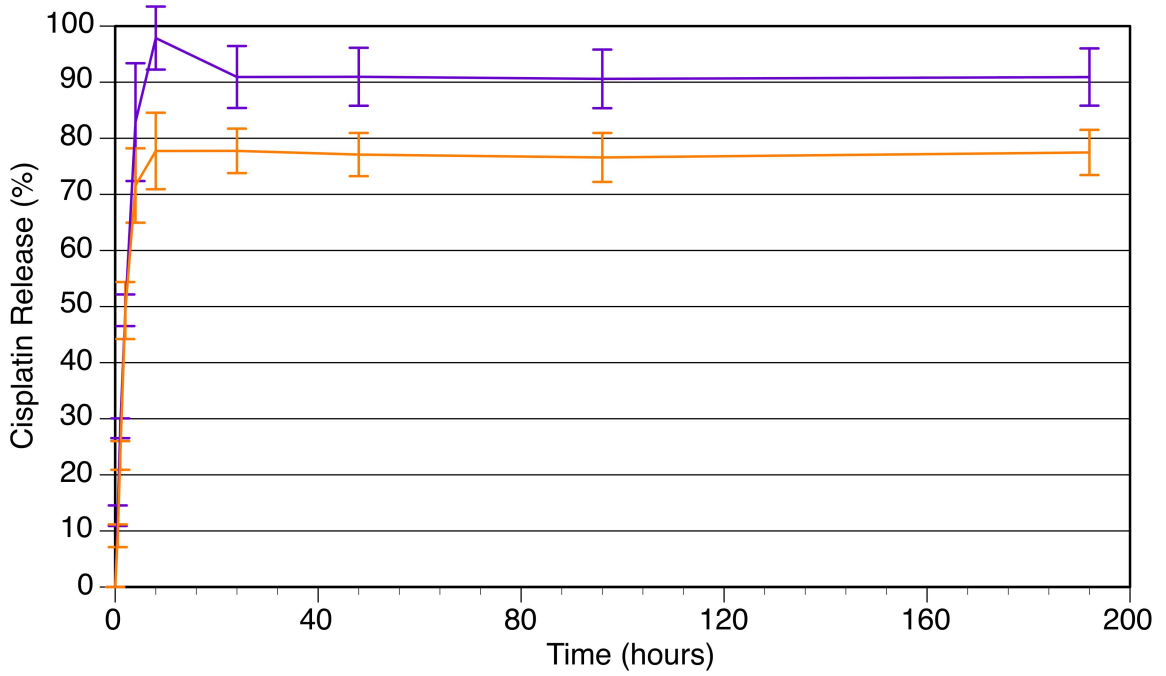
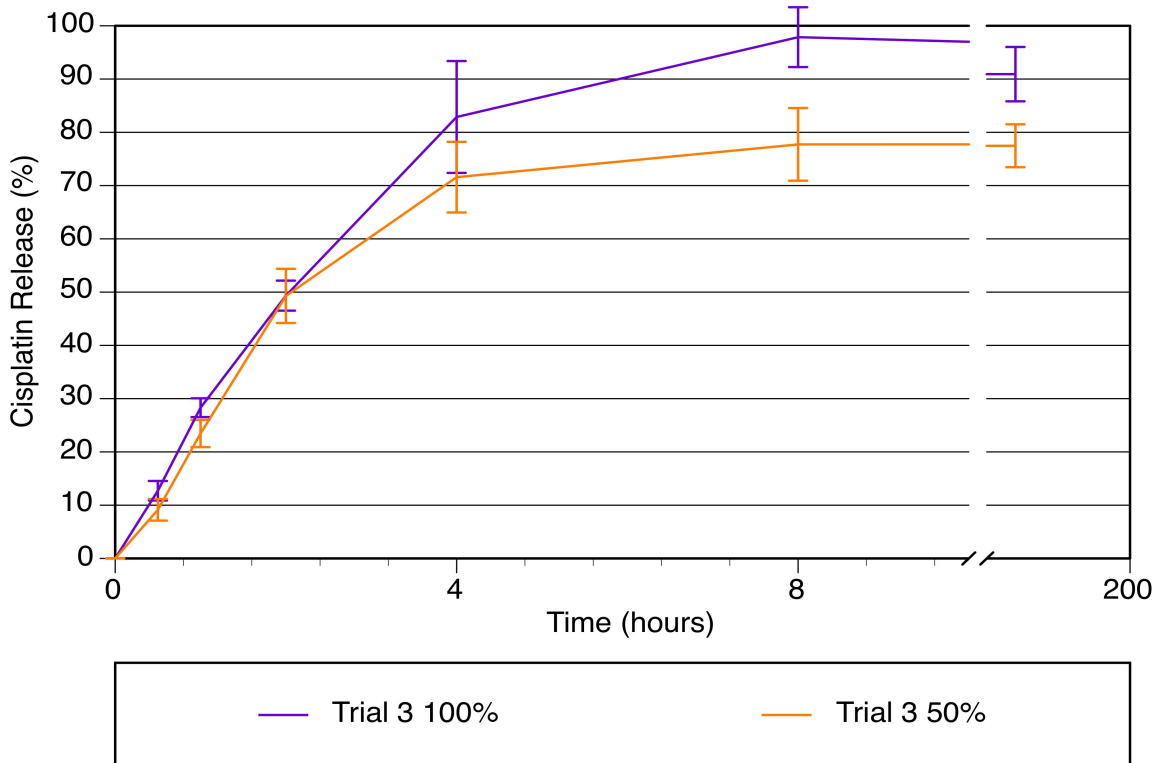


Figure 10b: Run 2, cumulative release of platinum over the first 8 hours of elution including end point.

Platinum release during run 3 demonstrated a rapid and profound burst release (Figure 11). The 100% loaded disks demonstrated 82.8% +/- 10.5 of the predicted platinum released within the first 4 hours, while the 50% loaded disks released 71.6% +/- 6.6 in the same time period. The total predicted load of platinum within the 100% loaded disks and 50% disks was 0.19 μ g/mg and 0.10 μ g/mg, respectively. After 192 hours, 91.9% +/- 5.1 and 77.5% +/- 4.0 of the predicted platinum was released from the 100% and 50% loaded disks respectively; 108.6% +/- 5.6 of predicted platinum was recovered from the 100% loaded disks and 101.1% +/- 4.2 was recovered from the 50% disks. The release rates were similar for the first 4 hours where the curves overlap, diverging for the remainder of the elution study.



(a)



(b)

Figure 11: Run 3 elution; a) Cumulative release data as represented by % of predicted cisplatin released over time. b) Cumulative release data for 0-8 hours plus endpoint data.

For the elution involving the miniaturized beads, slight expansion of the beads during the first two hours was observed (Figure 12); the resulting increase in size was approximately maintained throughout the remainder of the run. The beads would intermittently stick together, but none of the pairs remained conjoined for more than a few revolutions. The elution media became slightly cloudy after the first hour and the turbidity remained throughout the elution.

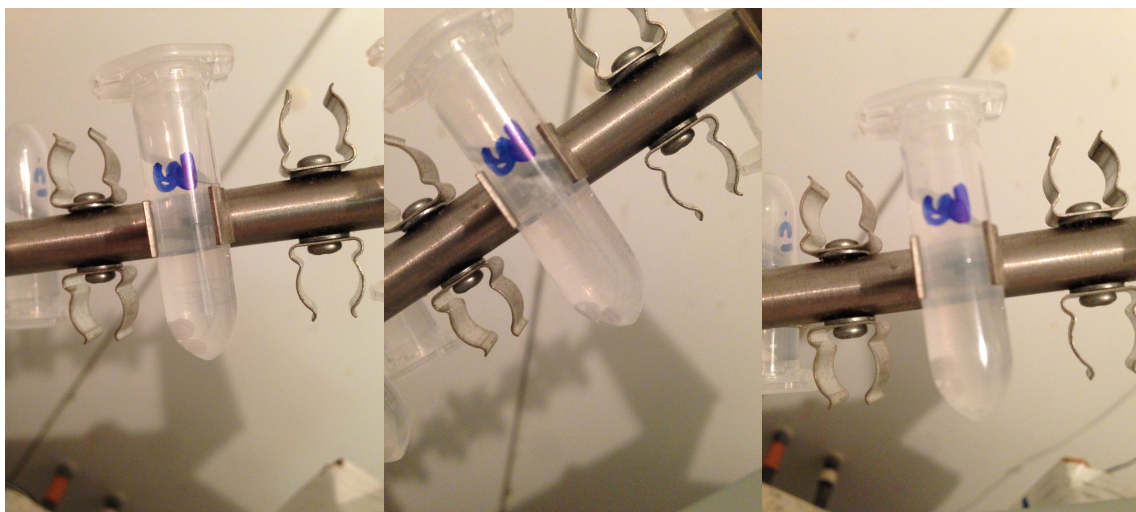
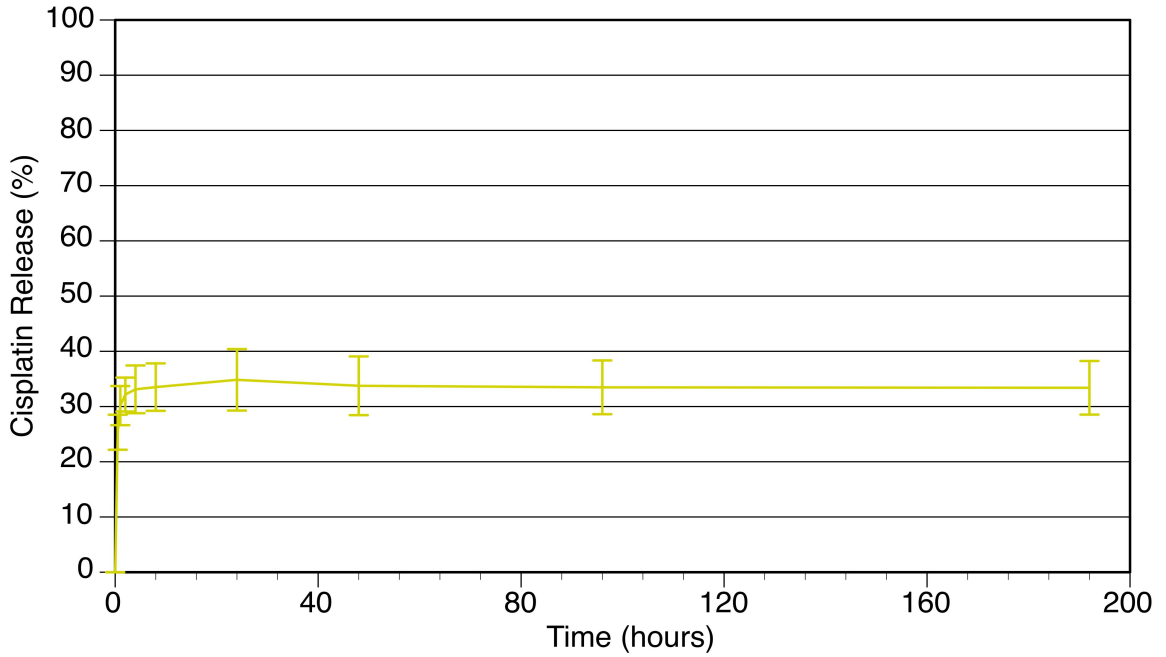
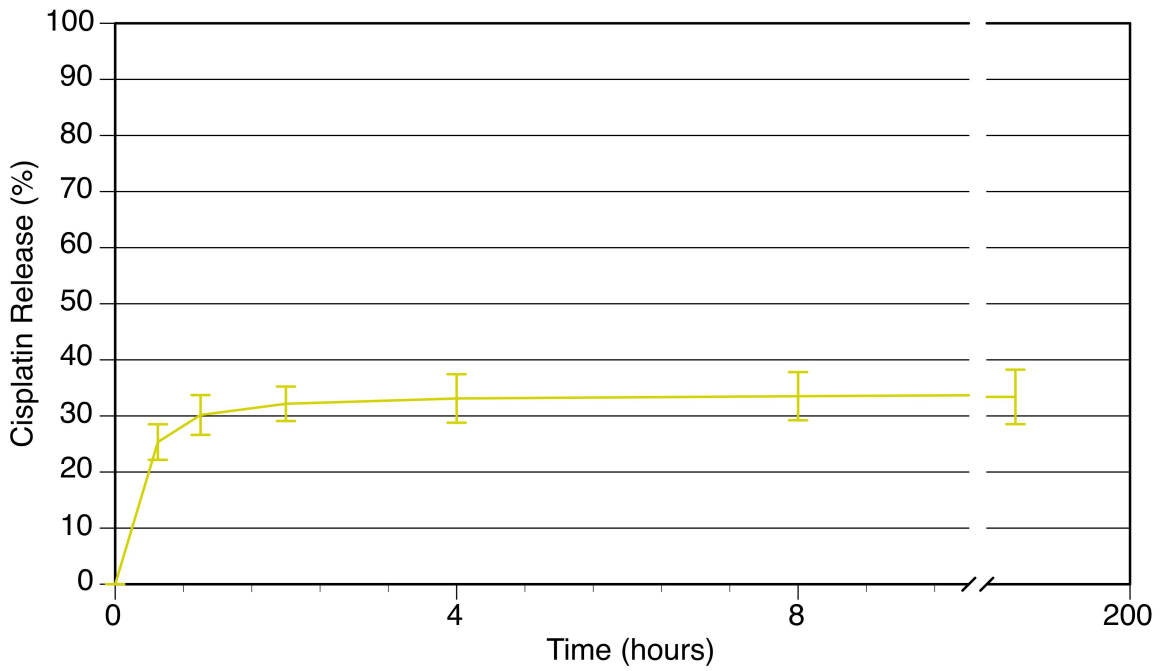


Figure 12: Digital images of the miniaturized elution with two cisplatin-loaded pellets. From left to right: 30 minutes; at 2 hrs; at 192 hrs.

The predicted platinum load within the G2 pellets was $0.17\mu\text{g}/\text{mg}$. Within the first 30 minutes there was a rapid burst release of $25.3\% \pm 2.9$ (Figure 13). The release rate slowed until 4 hours, at which point $33.1\% \pm 4.3$ of the predicted cisplatin was released. Over the next 188 hours no further release was noted, and at 192 hours there was a cumulative release of $33.4\% \pm 4.8$. Following completion of the elution study the remaining pellets were dissolved and $105.4\% \pm 7.4$ of the predicted cisplatin was recovered.

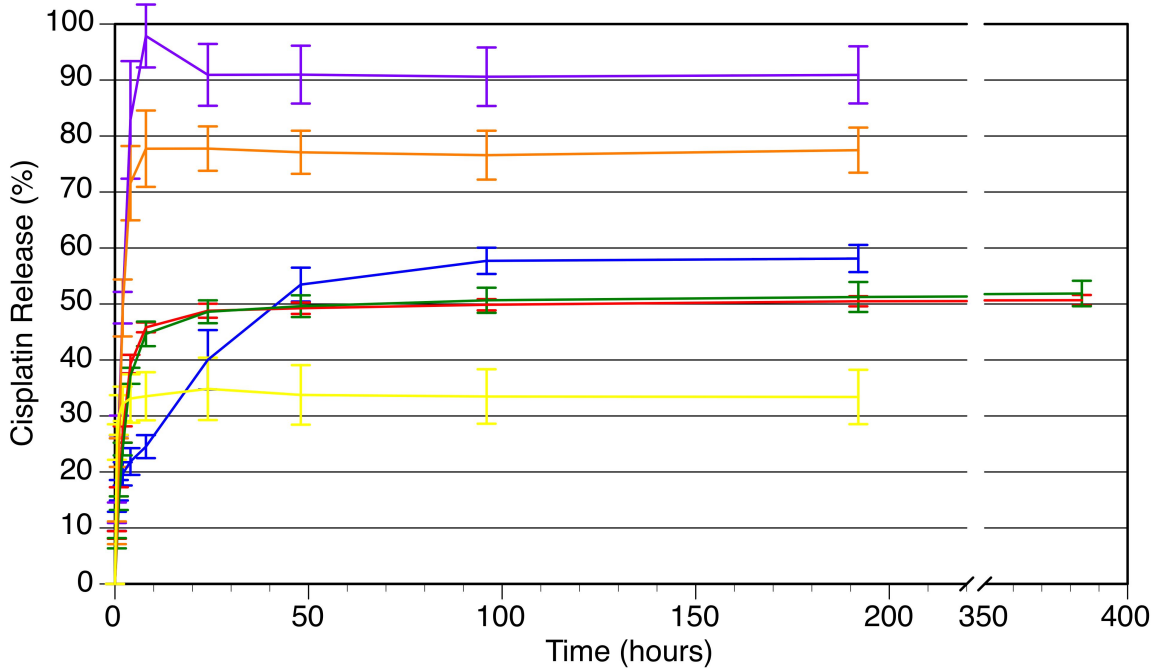


(a)

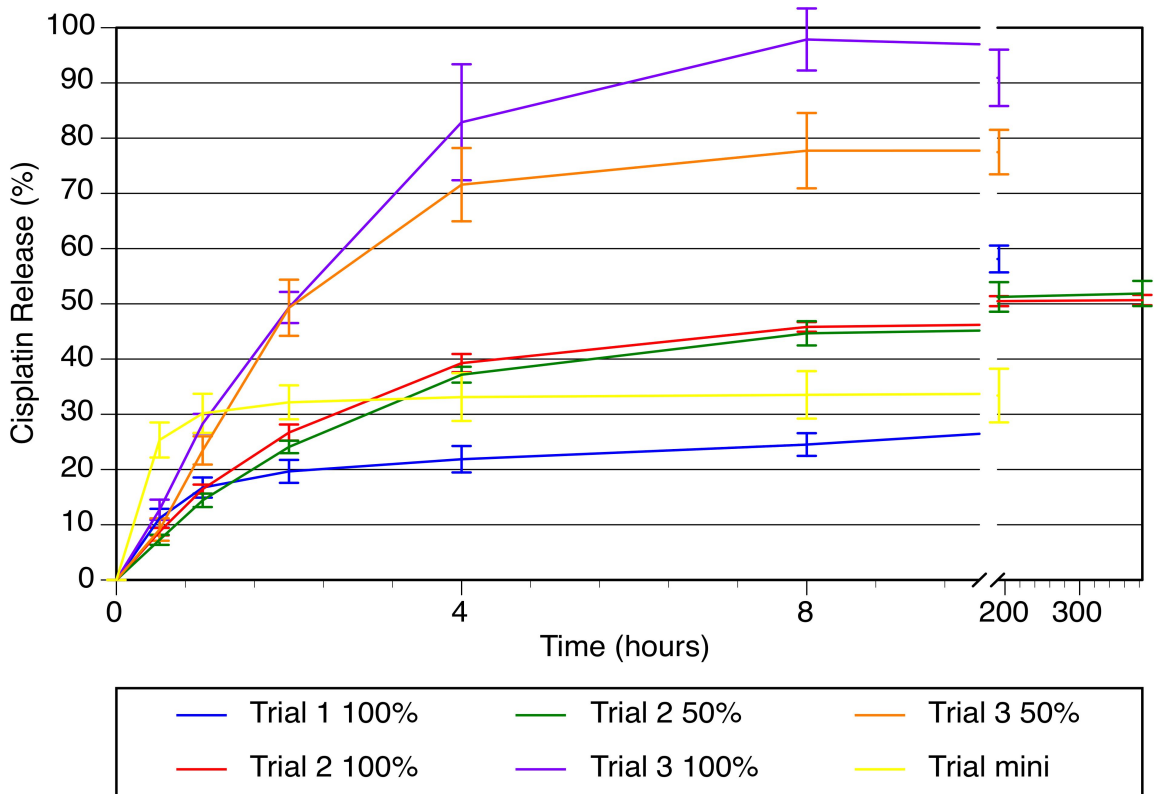


(b)

Figure 13: Miniaturized elution with cisplatin loaded pellets. a) Cumulative release of cisplatin from 0-192 hours. b) Cumulative release of cisplatin from the G2 pellets from 0-8 hours with end point included.



(a)



(b)

Figure 14: a) Combined elution data (Runs 1-3 plus miniaturized cisplatin pellet elution). b) From 0-8 hours, including end point.

3.4 CPP MATRIX DENSITY

Greater visual consistency overall was observed for the CIP processed samples compared to those produced by the established G2 protocol using uniaxial compaction (Figure 13). All of the CIP processed pellets had uniform shape and surface texture, while the axial pressed disks had irregularities in both shape and surface texture following gelling. The average apparent density of the CIP processed pellets was 2.29mg/mm³, while the average apparent density of the axial pressed disks was 1.7mg/mm³, or only 74% of the CIP pellets. The density of the CIP processed samples was significantly higher than that of the axial pressed samples (p<0.001).

Table 2: Density of axial pressed disks and CIP processed pellets

Sample	Mass (mg)	Dimension (mm)	Volume (mm ³)	Density (mg/mm ³)
Disk 1	127	7.5 x 1.8	79.52	1.60
Disk 2	131	7.5 x 1.7	75.10	1.74
Disk 3	125	7.4 x 1.7	73.11	1.71
Disk 4	129	7.5 x 1.8	79.52	1.62
Disk 5	131	7.5 x 1.6	70.69	1.85
Disk 6	128	7.5 x 1.7	75.10	1.70
Disk 7	134	7.5 x 1.8	79.52	1.68
Pellet 1	7.1	1.8 d	3.05	2.33
Pellet 2	7.0	1.8 d	3.05	2.29
Pellet 3	7.9	1.9 d	3.59	2.20
Pellet 4	7.1	1.8 d	3.05	2.33
Pellet 5	7.8	1.9 d	3.59	2.17
Pellet 6	7.9	1.9 d	3.05	2.59
Pellet 7	7.7	1.9 d	3.59	2.14



Figure 15: Digital image of a G2 axial pressed disk and a G2 CIP processed pellet.

3.5 CISPLATIN ACTIVITY

Hypothesis 3 stated that the cisplatin would continue to be active following incorporation into the CPP matrix. Following a 12-hour elution of 100% loaded G2 disks, the concentrations of cisplatin released (based on the measured platinum concentrations) were 9.51ppm, 9.17ppm and 9.49ppm. Each of these solutions was diluted by 50%, resulting in cisplatin concentrations of 4.75ppm, 4.58ppm and 4.75ppm. The resultant cisplatin solutions were tested against L1210 murine leukemia cells by MTT assay and compared to positive controls of fresh cisplatin solutions. The fresh cisplatin solutions were at concentrations of 15.4ppm, 11.5ppm, 7.7ppm and 3.8ppm, and were used to develop a control curve to which the test solutions could be compared (Figure 14). Table 3 shows the % viability of L1210 cells following 24 hours incubation with all of the test solutions.

Table 3: MTT assay results comparing both positive control and test solutions to the % viability

Sample	Pt PPM	Cisplatin PPM	% Viability
Test 1 – 100%	6.18	9.51	28.4
Test 2 – 100%	5.96	9.17	20.1
Test 3 – 100%	6.17	9.49	34.5
Test 1 – 50%	3.09	4.75	55.2
Test 2 – 50%	2.98	4.58	74.9
Test 3 – 50%	3.09	4.75	84.7
Pos Control	10	15.38	9.2
Pos Control	7.5	11.54	20.8
Pos Control	5	7.69	50.0
Pos Control	2.5	3.84	78.1
Neg Control	0	0	100

There was no significant difference in the variability of cellular response inherent in the 50% diluted test solutions, with resultant lower concentrations of cisplatin, when compared to the undiluted test solutions ($p=0.260$). At full concentration all of the test samples fell below the control curve, demonstrating greater cellular inhibition than the non-eluted (“fresh”) cisplatin. At lower concentrations there was some inhibition of the L1210 cells, all having a lower % viability than the negative control, with one of the test samples falling below the control curve and two slightly above the curve. The blank CPP disks also demonstrated growth inhibition, with the undiluted elution media demonstrating a lower cell viability (45%-50%) than the diluted control media (72%-80%) suggesting that the CPP itself was contributing to the observed cytotoxicity of the cisplatin. The 100% loaded solution was significantly more cytotoxic than the 100% blank solution ($p=0039$). Overall, cisplatin activity appeared to be retained following processing.

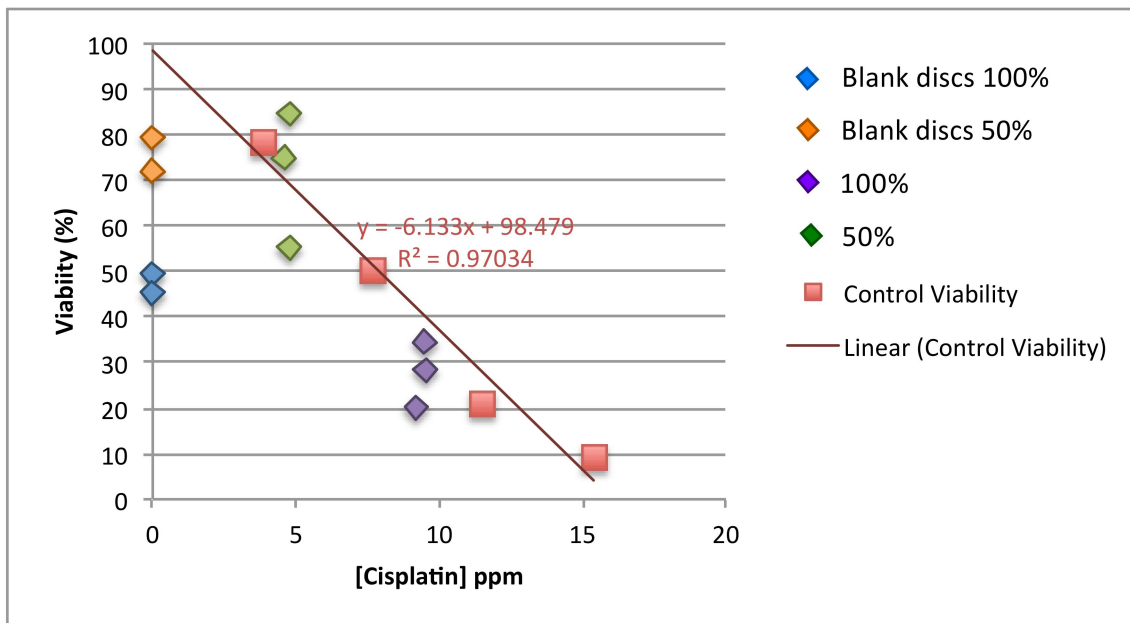


Figure 16: MTT assay comparing test solutions with control curve developed with fresh cisplatin solutions.

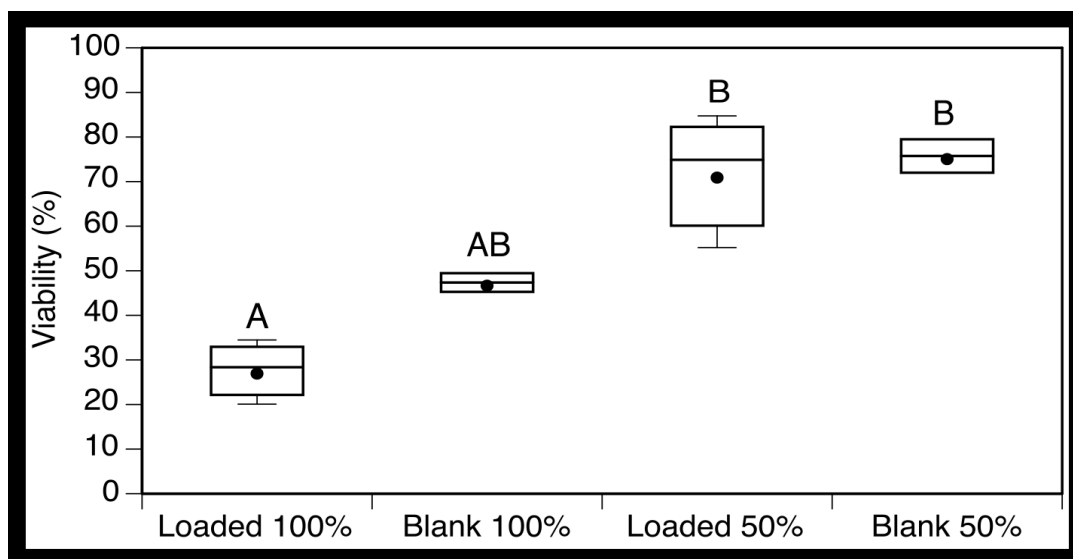


Figure 17: One-way ANOVA plot demonstrating the differences between the test and control groups in the MTT assay against L1210 cells

CHAPTER 4 DISCUSSION

A localized drug delivery system has to meet several requirements, including the predictable loading of a drug at a clinically effective dosage, the ability of the drug to maintain its therapeutic effects throughout the manufacturing process, and the sustained release of the drug into an aqueous environment. Ultimately, the goal of these systems is to deliver the drug to the desired tissues while limiting their systemic distribution.

Localized delivery systems can be particularly attractive for administering chemotherapeutic agents, as the systemic toxicity of these agents can limit the ability to deliver sufficient concentrations of the drug to the target tissues. Cisplatin is a prime example of an effective anti-tumor agent that interacts with non-cancerous cells to produce secondary effects, most notably neuro-,oto-, hepato- and nephrotoxicity; these limit the dose that can be delivered and make cisplatin an ideal candidate for localized delivery. The ideal release profile for a cisplatin delivery system is difficult to predict. However, an initial burst to reach therapeutic drug concentrations within the target tissues quickly followed by slow release to maintain these levels may prove to be an effective treatment strategy.

4.1 CISPLATIN LOADING INTO CPP MATRIX

The initial challenge of developing a drug delivery system is the loading of the therapeutic agent into the matrices in a predictable manner. Historically, cisplatin has proven to be a difficult molecule to manipulate when incorporating into other systems due to its physiochemical characteristics, poor solubility in water (1 mg/mL) and

degradability (83-85). Reconstituted cisplatin is only stable for 6 hours when exposed to UV light and thus requires fresh stock solutions be prepared immediately prior to each experiment. When attempting to load cisplatin into hydroxyapatite crystals, Barroug and Glimcher were only able to achieve binding of 22-25% of the available cisplatin (60). Subsequent work demonstrated that the loading of HA nanoparticles at room temperature varied from 20% – 25% but could be improved by 3 – 3.5 times by increasing the temperature from 24°C to 37°C (65).

In preliminary studies we had difficulty with poor consistency, low cisplatin uptake and recovery when stock solutions utilized NaCl as the solvent. A review of the available literature suggested that the absence of chloride was essential for cisplatin adsorption into calcium phosphate matrices (60). By utilizing deionized water we have demonstrated predictable and dose dependent loading of cisplatin into these long chain CPP matrices. Drug uptake into our delivery system ranged between 72% of available cisplatin for G2 disks processed from a 100% saturated cisplatin solution, and 75% for a 50% saturated solution. Cisplatin incorporation from these solutions is not significantly different ($p=0.164$). These results confirm Hypothesis 1, that cisplatin can be loaded into the CPP matrix in an efficient and dose dependent manner. The grey discoloration of the G2 gelled disks may be explained by the utilization of the planetary ball mill composed of alumina. Cisplatin is known to react quickly with aluminum ions, forming a black precipitate, and this may account for the discoloration that we have observed. For future studies an alternate method of grinding materials will be required to rule out this phenomenon. An alternate theory is that the cisplatin within the disks has reacted with

the CPP material while in the gelling process, causing the platinum to precipitate and making it more visible.

Due to its low solubility, the total amount cisplatin available for release is limited by the concentration of the stock solutions utilized to fabricate the G1 disks. For all disks manufactured with saturated cisplatin solutions throughout the course of this research, the concentration of cisplatin ranged between 0.29 μg and 0.34 μg per mg of material. To put the cisplatin concentration into perspective, the systemic injection of 10 mg/kg free cisplatin produced tumor platinum concentrations of 0.014 $\mu\text{g}/\text{mg}$ of tumor tissue in a mouse model (32). Although it is impossible to predict the distribution of *in vivo* administration of this delivery system based on this current study, it may be possible that these intratumoral levels could be reached given the current loading parameters.

4.2 DRUG ELUTION

In general, solute diffusion, polymeric matrix swelling, and material degradation are suggested to be the main driving forces for solute transport from drug-containing ceramic matrices (86). These processes were witnessed in this study, with gradual swelling of the disks during elution followed by the extrusion of the gel-like core as the disks began to degrade. Within the first hour we observed burst release of cisplatin from the system that ranged from between 14.4% - 28.3%. This was in contrast to studies by Petrone et al., who demonstrated the elimination of the initial burst release of vancomycin when incorporated in the same delivery system as examined here (74). This may be explained by the differences in the molecular properties of cisplatin and vancomycin. Cisplatin is a

relatively small molecule with a molecular weight and pK_a of 300.045 and 5.06, respectively. In contrast, vancomycin has a molecular weight of 1485.7 and 6 charged domains with pK_a values ranging from 2.18-12. This suggests that the individual properties of different molecules influence the release kinetics with this delivery system and as such, cisplatin is likely not as tightly trapped within the long chain CPP. It has been further demonstrated through MRI-based characterization that vancomycin does not have any direct interaction with the CPP matrix; rather it is physically trapped within the system and released by a Fickian diffusion mechanism (76). Based on the release characteristics we have witnessed here, specifically in runs 1 and 2 where only 58.12% and 50.67% of the incorporated cisplatin was released respectively, there is suggestion of some interaction between the cisplatin and the CPP that limits solute diffusion and further influences release kinetics. The potential bonding characteristics between cisplatin and CPP should be examined by nuclear magnetic resonance or Fourier transform infrared spectroscopy in future studies. It is possible that the burst release observed is a result of the cisplatin being readily released from the surface of the disks due to the small size of the drug or preferential distribution of the drug to the periphery of the gelled matrix, prior to a stronger interaction of the cisplatin within the matrix as the disks hydrate and re-gel in the presence of the aqueous media. Run 2 was extended for an additional 7 days to see if there would be a secondary release of cisplatin but this was not observed, and the remainder of the loaded platinum was recovered when the residual matrices were dissolved.

In run 1 the initial burst release only lasted for the first hour and slowed to a relatively steady rate up to eight hours, slowing again for the remainder of the study. The release characteristics of Run 1 most closely resembles that seen in previous work on drug release from these CPP matrices (74). Runs 2 and 3 each demonstrated progressively longer burst release periods resulting in more cisplatin released earlier in the run. All of the samples were fabricated from the same batch of CPP base material over several months, suggesting that there is degradation of the material with aging or during processing. Run 1 was completed in the winter months when the relative humidity within the lab was very low. Runs 2 and 3 were fabricated in the spring and summer, respectively, with increasingly higher relative humidity. This system is vulnerable to loss of chain length with exposure to water (87), and when milling the material to a <45 μ m powder the large surface area to volume ratio allows for significant wetting in high humidity. There is also potential exposure of the prepared CPP powder to moisture contamination in the vacuum storage chamber, as the repeated opening of the vessel may have allowed humidification. The change in material behavior further supports the theory of decreased chain length as demonstrated by a loss of structural integrity in Runs 2 and 3, where the disks had progressively less swelling, indicative of shorter chain length (73), prior to collapse.

Run 2 exemplified the consistent dose dependent nature of cisplatin release from this system. As shown in Figure 10, almost identical release curves for the 100% and 50% loaded disks were obtained with similar cumulative release for all time points. Run 3 showed similar release characteristics for the 50% and 100% samples for the first 4

hours; however, at 8 hours the 100% disks continued to release up to almost 100% of their predicted cisplatin load. This may be explained by the theorized shorter chain lengths, as previously discussed, limiting the ability of the system to hold on to a higher concentration of the drug. Still, the relative predictability of cisplatin release as a function of loading suggests the potential to tune local drug administration in this manner.

The CIP processed G2 pellets behaved in a somewhat unexpected manner that was very different from that of G2 disks. It was anticipated that the two pellets within the eppendorf tube would quickly gel and fuse together into an irregular mass; in reality, the pellets remained distinct from each other, with very little change to their size and shape. The release characteristics of the pellets also differed from what was expected. There was a rapid burst release of 25% of loaded cisplatin within the first two hours, faster than any of the other elution runs, and further release of an additional 8% over the next two hours. The remainder of the loaded cisplatin was trapped within the pellets until the end of the elution and was recovered when the pellets were dissolved. The rapid burst release can be explained in part by the increase in the surface to volume ratio as the carrier becomes smaller and takes on a spherical shape. The retention of the majority of cisplatin may have been the result of increased compaction of the pellets compared to the disks. CIP provides a more efficient compaction of materials by applying pressure from all directions, resulting in a more uniform, less porous product than that achieved by a uniaxial compaction process (77). This is supported by the measured higher apparent densities for the G2 pellets ($2.29\text{mg}/\text{mm}^3$) compared to that obtained with the G2 disks ($1.7\text{mg}/\text{mm}^3$). As polymer dissolution involves two transport processes, solvent

diffusion and chain disentanglement, with more efficient compaction there may have been an inability of water to ingress into the core of the disk, thereby limiting both the diffusional and relaxational processes needed to release the drug.

The ideal release profile for a localized cisplatin delivery system is difficult to predict. However, an initial burst release may allow for rapid therapeutic drug concentrations within the target tissues, followed by slow release to maintain these levels. The benefit of exposure to continuous low-dose cisplatin within tumor tissue has been demonstrated in several studies (10, 18, 22, 54). Although we did not witness the release of cisplatin will occur at a steady rate without demonstrate burst release (Hypothesis 2), the release profile that was observed may ultimately prove to be an effective treatment strategy.

4.3 CISPLATIN ACTIVITY

Given that cisplatin solutions are only stable for about 24 hours following reconstitution (84), there were concerns that the cytotoxicity of the drug may be affected by the repeated wetting required in the manufacturing of the G2 disks. The activity of cisplatin against a murine L1210 cell line was confirmed following a twelve-hour elution in growth medium. The L1210 cell line was chosen because it is known to be susceptible to the cytotoxic effects of cisplatin at the concentrations that we achieved during elution (88). This cell line has also been well studied in the literature with respect to cisplatin, both in regard to its relative sensitivity to this drug as well as the ease with which it is transformed into a cisplatin-resistant cell line (78, 80, 81, 89).

The assays completed with freshly dissolved cisplatin at the highest solution dose (15.4 μ g/ml) demonstrated the greatest cytotoxicity toward the L1210 cells. A dose dependent effect was observed for the lower doses of fresh cisplatin, creating a standard curve with which the measured concentrations of eluted cisplatin could be compared. When examining the cisplatin-loaded disks, growth inhibition of L1210 cells was witnessed with the higher concentration, non-diluted elution media. All of the samples in these groups showed similar or lower cell viability than the standard curve created by roughly equivalent fresh cisplatin concentrations, suggesting release of active cisplatin. The increase in potency over the predicted cytotoxicity for fresh cisplatin can be accounted for by the direct cytotoxic effect of the CPP matrix as was observed in the blank control disks. This has been witnessed in other cisplatin delivery systems, where the free cisplatin has proven less cytotoxic than that loaded into PLGA-mPEG nanoparticles (31). When the elution samples were diluted 50% there was continued cellular inhibition at a level similar to the control curve of fresh cisplatin: however, the cytotoxicity was also similar to that of blank CPP disks. Although there was continued growth inhibition in this group, the similarity to the diluted negative control samples suggests that there may have been some loss of drug activity throughout the processing or elution stages. It is difficult to extrapolate the degree of inhibition from the CPP and that from cisplatin. It is possible that although there is still cytotoxic activity of the drug it is masked by the CPP's cytotoxicity until the concentration of cisplatin is high enough to inhibit growth beyond that of the matrix itself. Further replication of these cytotoxicity studies must be completed to definitively answer to what extent, if any, there was a loss of cisplatin cytotoxic activity.

4.4 CLINICAL RELEVANCE/APPLICATION

The limiting factor for this delivery system when applied to cisplatin is the relatively low solubility of cisplatin in water (1mg/mL). Currently, when loading of a drug into the CPP powder during G1 processing only 60.2 μ L of solution is integrated into 150mg of CPP powder; at 1mg/mL the total available cisplatin for integration into the matrix is 60.2 μ g per disk or 0.40 μ g/mg of CPP. Despite this system demonstrating cytotoxicity *in vitro* there are limitations in making a leap to assumptions regarding its *in vivo* effectiveness. With the current loading strategy the volume of material required to reach a clinically effective dose may make implantation at the tumor site impractical. Only with *in vivo* studies will we be able to determine if this system has sufficient active cisplatin to sensitize SCC to ionizing radiation. There is potential to investigate other solvents when dissolving cisplatin, including dimethylformamide (DMF) in which cisplatin has a solubility of 16mg/mL and is stable in solution (85). Cisplatin had been dissolved in DMSO at a concentration of 10mg/mL for incorporation into a silica-calcium-phosphate nanocomposite to achieve 14.2mg cisplatin/g of material (68). Other loading strategies may also be explored, including adding solid-state cisplatin to CPP in the initial milling phase or during preparation of the G1 disks.

The ability to easily implant a drug delivery system is paramount to clinical applicability. We investigated cold isostatic pressing (CIP) in hopes of developing a miniaturized system that could be introduced with minimal invasiveness into a tumor bed. CIP allows for the manufacturing of a very dense product in virtually any size or shape. We developed a 1.7-1.8 mm sphere or pellet that could be introduced by trocar in a system

similar to that used for the introduction of sub-dermal contraceptive devices; the potential exists to further reduce pellet size through CIP. Overall, this system would allow for guided placement of the pellets under fluoroscopy insuring that the target tissues are reached.

CHAPTER 5 LIMITATIONS AND FUTURE WORK

5.1 LIMITATIONS

To date the body of work surrounding CPP as a drug delivery system is based on *in vitro* studies. Until *in vivo* studies are available it is difficult to draw conclusions on the clinical behavior of the system. Some of the variables that have not been accounted for include, but are not limited to, enzymatic and cellular breakdown of the CPP matrix, placement of the material into a confined space and limited fluid ingress. We presume that matrix hydration, swelling and degradation will be significantly affected *in vivo*.

The decision to use the same CPP base material batch throughout all of the experiments within this work was based on a desire to maintain consistency. We did not predict that there would be material degradation over time, an assumption here given that we did not characterize the material (specifically, chain length) throughout the length of the study. Given the results that were witnessed, a new batch of CPP should be produced prior to each experiment to remove this variable.

While we did demonstrate some retention of cisplatin activity following elution from the G2 disks, we did not confirm that similar activity was retained for the CIP-processed matrices.

Finally, CIP elution and MTT assay analyses were compromised in part by low statistical power; increased sample numbers should be considered in any future analyses.

5.2 FUTURE WORK

The optimization of drug loading to increase the concentration of cisplatin within the system would be of clinical benefit. This may be achieved by adding solid-state cisplatin to the CPP powder prior to hydration or dissolving cisplatin in an organic solvent such as DMSO prior to G1 disc fabrication. Although difficult to predict based on *in vitro* studies, the current concentration of cisplatin within the matrix may require excessive quantities of matrix be implanted to achieve therapeutic drug concentrations. Examining the distribution of the drug within the system may demonstrate why we have seen more pronounced burst release than expected.

Based on the varied results observed in our elution runs, investigating the effects of material aging, humidity and moisture contamination on chain length and the subsequent ability to deliver cisplatin is warranted.

The ability to manipulate the CIP parameters (time and pressure and bead size) should allow fine-tuning of the release characteristics from this system. By customizing the delivery system in this manner, a suitable release profile can potentially be tailored to tumors of various type and location. *In vivo* studies are required to determine the cellular and enzymatic effects on material decomposition and drug release for any future studies seeking to adjust the release characteristics of the CPP matrix.

CHAPTER 6 CONCLUSION

The foreseeable future of advanced SCC treatment of the head and neck will include surgical, chemical and ionizing therapy. The ability to deposit cytotoxic therapy in the vicinity of a tumor bed allows for high local concentrations of the drug while minimizing systemic toxicity. In the current study we have presented a calcium polyphosphate cisplatin delivery matrix that demonstrated some predictable and unexpected results. A predictable and dose dependent loading of the drug was demonstrated as well as the ability of the material to release cisplatin over time; in this study, however, we were not able to demonstrate consistency during elution, an issue that may be tied to aging of the stock material or due to the interaction of the drug with the CPP. Following material processing, cisplatin maintains at least some of its cytotoxic profile at higher concentrations, although clinically effective dosaging is difficult to predict based on *in vitro* study. The ability to process the material using CIP to create an implantable size while still maintaining a degree of delayed release improves the clinical applicability of the system.

Further investigation of CPP as a drug delivery system for cisplatin is warranted to optimise loading of the drug at higher concentrations, fine tune the release characteristics of both the G2 disk and CIP processed materials and analyze the effects of aging, humidity and moisture contamination of the CPP.

BIBLIOGRAPHY

1. Kamangar F, Dores GM, Anderson WF. Patterns of cancer incidence, mortality, and prevalence across five continents: defining priorities to reduce cancer disparities in different geographic regions of the world. *Journal of clinical oncology : official journal of the American Society of Clinical Oncology*. 2006 May 10;24(14):2137-50. PubMed PMID: 16682732.
2. Shibuya K, Mathers CD, Boschi-Pinto C, Lopez AD, Murray CJ. Global and regional estimates of cancer mortality and incidence by site: II. Results for the global burden of disease 2000. *BMC Cancer*. 2002 Dec 26;2:37. PubMed PMID: 12502432. Pubmed Central PMCID: 149364.
3. D'Souza G, Kreimer AR, Viscidi R, Pawlita M, Fakhry C, Koch WM, et al. Case-control study of human papillomavirus and oropharyngeal cancer. *The New England journal of medicine*. 2007 May 10;356(19):1944-56. PubMed PMID: 17494927.
4. Forastiere AA. Head and neck cancer: overview of recent developments and future directions. *Semin Oncol*. 2000 Aug;27(4 Suppl 8):1-4. PubMed PMID: 10952432.
5. Price KA, Cohen EE. Current treatment options for metastatic head and neck cancer. *Curr Treat Options Oncol*. 2012 Mar;13(1):35-46. PubMed PMID: 22252884.
6. Gil Z, Fliss DM. Contemporary management of head and neck cancers. *Isr Med Assoc J*. 2009 May;11(5):296-300. PubMed PMID: 19637508.
7. Yao M, Epstein JB, Modi BJ, Pytynia KB, Mundt AJ, Feldman LE. Current surgical treatment of squamous cell carcinoma of the head and neck. *Oral Oncol*. 2007 Mar;43(3):213-23. PubMed PMID: 16978911.
8. Varkey P, Liu YT, Tan NC. Multidisciplinary treatment of head and neck cancer. *Semin Plast Surg*. 2010 Aug;24(3):331-4. PubMed PMID: 22550455. Pubmed Central PMCID: 3324236.
9. Pignon JP, le Maitre A, Maillard E, Bourhis J, Group M-NC. Meta-analysis of chemotherapy in head and neck cancer (MACH-NC): an update on 93 randomised trials and 17,346 patients. *Radiotherapy and oncology : journal of the European Society for Therapeutic Radiology and Oncology*. 2009 Jul;92(1):4-14. PubMed PMID: 19446902.
10. Mitsudo K, Shigetomi T, Fujimoto Y, Nishiguchi H, Yamamoto N, Furue H, et al. Organ preservation with daily concurrent chemoradiotherapy using superselective intra-arterial infusion via a superficial temporal artery for T3 and T4 head and neck cancer. *International journal of radiation oncology, biology, physics*. 2011 Apr 1;79(5):1428-35. PubMed PMID: 20605340.
11. Smee RI, Broadley K, Bridger GP, Williams J. Floor of mouth carcinoma: surgery still the dominant mode of treatment. *J Med Imaging Radiat Oncol*. 2012 Jun;56(3):338-46. PubMed PMID: 22697334.
12. Spector JG, Sessions DG, Chao KS, Hanson JM, Simpson JR, Perez CA. Management of stage II (T2N0M0) glottic carcinoma by radiotherapy and conservation surgery. *Head & neck*. 1999 Mar;21(2):116-23. PubMed PMID: 10091979.
13. Seiwert TY, Cohen EE. State-of-the-art management of locally advanced head and neck cancer. *Br J Cancer*. 2005 Apr 25;92(8):1341-8. PubMed PMID: 15846296. Pubmed Central PMCID: 2361996.
14. Ma J, Liu Y, Huang XL, Zhang ZY, Myers JN, Neskey DM, et al. Induction chemotherapy decreases the rate of distant metastasis in patients with head and neck

- squamous cell carcinoma but does not improve survival or locoregional control: A meta-analysis. *Oral Oncol.* 2012 Nov;48(11):1076-84. PubMed PMID: 22800881.
15. Kirita T, Yamanaka Y, Imai Y, Yamakawa N, Aoki K, Nakagawa Y, et al. Preoperative concurrent chemoradiotherapy for stages II-IV oral squamous cell carcinoma: a retrospective analysis and the future possibility of this treatment strategy. *Int J Oral Maxillofac Surg.* 2012 Apr;41(4):421-8. PubMed PMID: 22356740.
 16. Budach W, Hehr T, Budach V, Belka C, Dietz K. A meta-analysis of hyperfractionated and accelerated radiotherapy and combined chemotherapy and radiotherapy regimens in unresected locally advanced squamous cell carcinoma of the head and neck. *BMC Cancer.* 2006;6:28. PubMed PMID: 16448551. Pubmed Central PMCID: 1379652.
 17. Fury MG, Pfister DG. Current recommendations for systemic therapy of recurrent and/or metastatic head and neck squamous cell cancer. *J Natl Compr Canc Netw.* 2011 Jun 1;9(6):681-9. PubMed PMID: 21636539.
 18. Kumar P, Robbins KT. Treatment of advanced head and neck cancer with intra-arterial cisplatin and concurrent radiation therapy: the 'RADPLAT' protocol. *Current oncology reports.* 2001 Jan;3(1):59-65. PubMed PMID: 11123871.
 19. Hehr T, Classen J, Welz S, Ganswindt U, Scheithauer H, Koitschev A, et al. Hyperfractionated, accelerated chemoradiation with concurrent mitomycin-C and cisplatin in locally advanced head and neck cancer, a phase I/II study. *Radiotherapy and oncology : journal of the European Society for Therapeutic Radiology and Oncology.* 2006 Jul;80(1):33-8. PubMed PMID: 16875750.
 20. Katori H, Tsukuda M. Comparison of induction chemotherapy with docetaxel, cisplatin, and 5-fluorouracil (TPF) followed by radiation vs concurrent chemoradiotherapy with TPF in patients with locally advanced squamous cell carcinoma of the head and neck. *Clin Oncol (R Coll Radiol).* 2005 May;17(3):148-52. PubMed PMID: 15900997.
 21. Budach V, Stuschke M, Budach W, Baumann M, Geismar D, Grabenbauer G, et al. Hyperfractionated accelerated chemoradiation with concurrent fluorouracil-mitomycin is more effective than dose-escalated hyperfractionated accelerated radiation therapy alone in locally advanced head and neck cancer: final results of the radiotherapy cooperative clinical trials group of the German Cancer Society 95-06 Prospective Randomized Trial. *Journal of clinical oncology : official journal of the American Society of Clinical Oncology.* 2005 Feb 20;23(6):1125-35. PubMed PMID: 15718308.
 22. Fuwa N, Kodaira T, Furutani K, Tachibana H, Nakamura T, Nakahara R, et al. Intra-arterial chemoradiotherapy for locally advanced oral cavity cancer: analysis of therapeutic results in 134 cases. *Br J Cancer.* 2008 Mar 25;98(6):1039-45. PubMed PMID: 18283309. Pubmed Central PMCID: 2275486.
 23. Robbins KT, Kumar P, Harris J, McCulloch T, Cmelak A, Sofferman R, et al. Supradose intra-arterial cisplatin and concurrent radiation therapy for the treatment of stage IV head and neck squamous cell carcinoma is feasible and efficacious in a multi-institutional setting: results of Radiation Therapy Oncology Group Trial 9615. *Journal of clinical oncology : official journal of the American Society of Clinical Oncology.* 2005 Mar 1;23(7):1447-54. PubMed PMID: 15735120.
 24. Fuwa N, Kodaira T, Furutani K, Tachibana H, Nakamura T, Daimon T. Chemoradiation therapy using radiotherapy, systemic chemotherapy with 5-fluorouracil

- and nedaplatin, and intra-arterial infusion using carboplatin for locally advanced head and neck cancer - Phase II study. *Oral Oncol.* 2007 Nov;43(10):1014-20. PubMed PMID: 17258494.
25. Prestwich RJ, Oksuz DC, Dyker K, Coyle C, Sen M. Feasibility and efficacy of induction docetaxel, cisplatin, and 5-fluorouracil chemotherapy combined with cisplatin concurrent chemoradiotherapy for nonmetastatic Stage IV head-and-neck squamous cell carcinomas. *International journal of radiation oncology, biology, physics.* 2011 Nov 15;81(4):e237-43. PubMed PMID: 21620580.
26. Su YX, Zheng JW, Zheng GS, Liao GQ, Zhang ZY. Neoadjuvant chemotherapy of cisplatin and fluorouracil regimen in head and neck squamous cell carcinoma: a meta-analysis. *Chin Med J (Engl).* 2008 Oct 5;121(19):1939-44. PubMed PMID: 19080128.
27. Bae WK, Hwang JE, Shim HJ, Cho SH, Lee JK, Lim SC, et al. Phase II study of docetaxel, cisplatin, and 5-FU induction chemotherapy followed by chemoradiotherapy in locoregionally advanced nasopharyngeal cancer. *Cancer chemotherapy and pharmacology.* 2010 Feb;65(3):589-95. PubMed PMID: 19830427.
28. Klopp CT, Alford TC, Bateman J, Berry GN, Winship T. Fractionated intra-arterial cancer; chemotherapy with methyl bis amine hydrochloride; a preliminary report. *Ann Surg.* 1950 Oct;132(4):811-32. PubMed PMID: 14771793. Pubmed Central PMCID: 1616816.
29. Lee YY, Wallace S, Dimery I, Goepfert H. Intraarterial chemotherapy of head and neck tumors. *AJNR American journal of neuroradiology.* 1986 Mar-Apr;7(2):343-8. PubMed PMID: 3082167.
30. Robbins KT, Storniolo AM, Kerber C, Vicario D, Seagren S, Shea M, et al. Phase I study of highly selective supradose cisplatin infusions for advanced head and neck cancer. *Journal of clinical oncology : official journal of the American Society of Clinical Oncology.* 1994 Oct;12(10):2113-20. PubMed PMID: 7931481.
31. Cheng L, Jin C, Lv W, Ding Q, Han X. Developing a highly stable PLGA-mPEG nanoparticle loaded with cisplatin for chemotherapy of ovarian cancer. *PLoS One.* 2011;6(9):e25433. PubMed PMID: 21966528. Pubmed Central PMCID: 3180455.
32. Shikanov A, Shikanov S, Vaisman B, Golenser J, Domb AJ. Cisplatin tumor biodistribution and efficacy after intratumoral injection of a biodegradable extended release implant. *Chemotherapy research and practice.* 2011;2011:175054. PubMed PMID: 22295203. Pubmed Central PMCID: 3265254.
33. Janne PA, Gray N, Settleman J. Factors underlying sensitivity of cancers to small-molecule kinase inhibitors. *Nat Rev Drug Discov.* 2009 Sep;8(9):709-23. PubMed PMID: 19629074.
34. Green MR. Targeting targeted therapy. *The New England journal of medicine.* 2004 May 20;350(21):2191-3. PubMed PMID: 15118072.
35. Aggarwal SK. A histochemical approach to the mechanism of action of cisplatin and its analogues. *J Histochem Cytochem.* 1993 Jul;41(7):1053-73. PubMed PMID: 8515048.
36. Ortega JA, Douglass EC, Feusner JH, Reynolds M, Quinn JJ, Finegold MJ, et al. Randomized comparison of cisplatin/vincristine/fluorouracil and cisplatin/continuous infusion doxorubicin for treatment of pediatric hepatoblastoma: A report from the Children's Cancer Group and the Pediatric Oncology Group. *Journal of clinical oncology*

- : official journal of the American Society of Clinical Oncology. 2000 Jul;18(14):2665-75. PubMed PMID: 10894865.
37. Daugaard G, Abildgaard U. Cisplatin nephrotoxicity. A review. *Cancer chemotherapy and pharmacology*. 1989;25(1):1-9. PubMed PMID: 2686850.
 38. Mukherjea D, Rybak LP. Pharmacogenomics of cisplatin-induced ototoxicity. *Pharmacogenomics*. 2011 Jul;12(7):1039-50. PubMed PMID: 21787192. Pubmed Central PMCID: 3217465.
 39. Rosenberg B, Vancamp L, Krigas T. Inhibition of Cell Division in Escherichia Coli by Electrolysis Products from a Platinum Electrode. *Nature*. 1965 Feb 13;205:698-9. PubMed PMID: 14287410.
 40. Hill JM, Loeb E, MacLellan A, Hill NO, Khan A, King JJ. Clinical studies of Platinum Coordination compounds in the treatment of various malignant diseases. *Cancer Chemother Rep*. 1975 May-Jun;59(3):647-59. PubMed PMID: 1203889.
 41. Sanchez-Gonzalez PD, Lopez-Hernandez FJ, Lopez-Novoa JM, Morales AI. An integrative view of the pathophysiological events leading to cisplatin nephrotoxicity. *Crit Rev Toxicol*. 2011 Nov;41(10):803-21. PubMed PMID: 21838551.
 42. Rades D, Ulbricht T, Hakim SG, Schild SE. Cisplatin superior to carboplatin in adjuvant radiochemotherapy for locally advanced cancers of the oropharynx and oral cavity. *Strahlenther Onkol*. 2012 Jan;188(1):42-8. PubMed PMID: 22194029.
 43. Boeckman HJ, Trego KS, Turchi JJ. Cisplatin sensitizes cancer cells to ionizing radiation via inhibition of nonhomologous end joining. *Molecular cancer research : MCR*. 2005 May;3(5):277-85. PubMed PMID: 15886299. Pubmed Central PMCID: 2432110.
 44. Sharma VM, Wilson WR. Radiosensitization of advanced squamous cell carcinoma of the head and neck with cisplatin during concomitant radiation therapy. *European archives of oto-rhino-laryngology : official journal of the European Federation of Oto-Rhino-Laryngological Societies*. 1999;256(9):462-5. PubMed PMID: 10552227.
 45. Steel GG, Peckham MJ. Exploitable mechanisms in combined radiotherapy-chemotherapy: the concept of additivity. *International journal of radiation oncology, biology, physics*. 1979 Jan;5(1):85-91. PubMed PMID: 422420.
 46. Bachaud JM, David JM, Boussin G, Daly N. Combined postoperative radiotherapy and weekly cisplatin infusion for locally advanced squamous cell carcinoma of the head and neck: preliminary report of a randomized trial. *International journal of radiation oncology, biology, physics*. 1991 Feb;20(2):243-6. PubMed PMID: 1991685.
 47. Bachaud JM, Cohen-Jonathan E, Alzieu C, David JM, Serrano E, Daly-Schweitzer N. Combined postoperative radiotherapy and weekly cisplatin infusion for locally advanced head and neck carcinoma: final report of a randomized trial. *International journal of radiation oncology, biology, physics*. 1996 Dec 1;36(5):999-1004. PubMed PMID: 8985019.
 48. Brizel DM, Albers ME, Fisher SR, Scher RL, Richtsmeier WJ, Hars V, et al. Hyperfractionated irradiation with or without concurrent chemotherapy for locally advanced head and neck cancer. *The New England journal of medicine*. 1998 Jun 18;338(25):1798-804. PubMed PMID: 9632446.
 49. Jeremic B, Shibamoto Y, Stanisavljevic B, Milojevic L, Milicic B, Nikolic N. Radiation therapy alone or with concurrent low-dose daily either cisplatin or carboplatin in locally advanced unresectable squamous cell carcinoma of the head and neck: a

- prospective randomized trial. *Radiotherapy and oncology : journal of the European Society for Therapeutic Radiology and Oncology*. 1997 Apr;43(1):29-37. PubMed PMID: 9165134.
50. Wong SJ, Harari PM, Garden AS, Schwartz M, Bellm L, Chen A, et al. Longitudinal Oncology Registry of Head and Neck Carcinoma (LORHAN): analysis of chemoradiation treatment approaches in the United States. *Cancer*. 2011 Apr 15;117(8):1679-86. PubMed PMID: 21472715.
 51. Bernier J, Cooper JS, Pajak TF, van Glabbeke M, Bourhis J, Forastiere A, et al. Defining risk levels in locally advanced head and neck cancers: a comparative analysis of concurrent postoperative radiation plus chemotherapy trials of the EORTC (#22931) and RTOG (# 9501). *Head & neck*. 2005 Oct;27(10):843-50. PubMed PMID: 16161069.
 52. de Castro G, Jr., Snitcovsky IM, Gebrim EM, Leitao GM, Nadalin W, Ferraz AR, et al. High-dose cisplatin concurrent to conventionally delivered radiotherapy is associated with unacceptable toxicity in unresectable, non-metastatic stage IV head and neck squamous cell carcinoma. *European archives of oto-rhino-laryngology : official journal of the European Federation of Oto-Rhino-Laryngological Societies*. 2007 Dec;264(12):1475-82. PubMed PMID: 17643256.
 53. Tsan DL, Lin CY, Kang CJ, Huang SF, Fan KH, Liao CT, et al. The comparison between weekly and three-weekly cisplatin delivered concurrently with radiotherapy for patients with postoperative high-risk squamous cell carcinoma of the oral cavity. *Radiation oncology*. 2012;7:215. PubMed PMID: 23245290. Pubmed Central PMCID: 3564896.
 54. Fuwa N, Kodaira T, Furutani K, Tachibana H, Nakamura T, Nakahara R, et al. Arterial chemoradiotherapy for locally advanced tongue cancer: analysis of retrospective study of therapeutic results in 88 patients. *International journal of radiation oncology, biology, physics*. 2008 Nov 15;72(4):1090-100. PubMed PMID: 18411003.
 55. Miura S, Mii Y, Miyauchi Y, Ohgushi H, Morishita T, Hohnoki K, et al. Efficacy of slow-releasing anticancer drug delivery systems on transplantable osteosarcomas in rats. *Jpn J Clin Oncol*. 1995 Jun;25(3):61-71. PubMed PMID: 7596050.
 56. Wolinsky JB, Liu R, Walpole J, Chirieac LR, Colson YL, Grinstaff MW. Prevention of in vivo lung tumor growth by prolonged local delivery of hydroxycamptothecin using poly(ester-carbonate)-collagen composites. *J Control Release*. 2010 Jun 15;144(3):280-7. PubMed PMID: 20184934.
 57. Lebugle A, Rodrigues A, Bonneville P, Voigt JJ, Canal P, Rodriguez F. Study of implantable calcium phosphate systems for the slow release of methotrexate. *Biomaterials*. 2002 Aug;23(16):3517-22. PubMed PMID: 12099297.
 58. Uchida A, Shinto Y, Araki N, Ono K. Slow release of anticancer drugs from porous calcium hydroxyapatite ceramic. *J Orthop Res*. 1992 May;10(3):440-5. PubMed PMID: 1314896.
 59. Tahara Y, Ishii Y. Apatite cement containing cis-diamminedichloroplatinum implanted in rabbit femur for sustained release of the anticancer drug and bone formation. *J Orthop Sci*. 2001;6(6):556-65. PubMed PMID: 11793179.
 60. Barroug A, Glimcher MJ. Hydroxyapatite crystals as a local delivery system for cisplatin: adsorption and release of cisplatin in vitro. *J Orthop Res*. 2002 Mar;20(2):274-80. PubMed PMID: 11918306.

61. Bray JM, Petrone C, Filiaggi M, Beyea SD. Measurement of fluid ingress into calcium polyphosphate bioceramics using nuclear magnetic resonance microscopy. *Solid State Nucl Magn Reson*. 2007 Dec;32(4):118-28. PubMed PMID: 17996428.
62. Benghuzzi HA, England BG, Bajpai PK. Controlled release of hydrophilic compounds by resorbable and biodegradable ceramic drug delivery devices. *Biomed Sci Instrum*. 1992;28:179-82. PubMed PMID: 1322731.
63. Guicheux J, Grimandi G, Trecant M, Faivre A, Takahashi S, Daculsi G. Apatite as carrier for growth hormone: in vitro characterization of loading and release. *J Biomed Mater Res*. 1997 Feb;34(2):165-70. PubMed PMID: 9029295.
64. Bajpai PK, Benghuzzi HA. Ceramic systems for long-term delivery of chemicals and biologicals. *J Biomed Mater Res*. 1988 Dec;22(12):1245-66. PubMed PMID: 3235459.
65. Barroug A, Kuhn LT, Gerstenfeld LC, Glimcher MJ. Interactions of cisplatin with calcium phosphate nanoparticles: in vitro controlled adsorption and release. *J Orthop Res*. 2004 Jul;22(4):703-8. PubMed PMID: 15183424.
66. Peng J, Qi T, Liao J, Chu B, Yang Q, Li W, et al. Controlled release of cisplatin from pH-thermal dual responsive nanogels. *Biomaterials*. 2013 Nov;34(34):8726-40. PubMed PMID: 23948167.
67. Fan W, Shen B, Bu W, Chen F, Zhao K, Zhang S, et al. Rattle-structured multifunctional nanotheranostics for synergetic chemo-/radiotherapy and simultaneous magnetic/luminescent dual-mode imaging. *J Am Chem Soc*. 2013 May 1;135(17):6494-503. PubMed PMID: 23574400.
68. Swet JH, Pacheco HJ, Iannitti DA, El-Ghanam A, McKillop IH. A silica-calcium-phosphate nanocomposite drug delivery system for the treatment of hepatocellular carcinoma: In vivo study. *Journal of biomedical materials research Part B, Applied biomaterials*. 2013 Aug 1. PubMed PMID: 23913418.
69. Pilliar RM, Filiaggi MJ, Wells JD, Grynblas MD, Kandel RA. Porous calcium polyphosphate scaffolds for bone substitute applications -- in vitro characterization. *Biomaterials*. 2001 May;22(9):963-72. PubMed PMID: 11311015.
70. Fukui H, Taki Y, Abe Y. Implantation of new calcium phosphate glass-ceramics. *J Dent Res*. 1977 Oct;56(10):1260. PubMed PMID: 272391.
71. Dion A, Langman M, Hall G, Filiaggi M. Vancomycin release behaviour from amorphous calcium polyphosphate matrices intended for osteomyelitis treatment. *Biomaterials*. 2005 Dec;26(35):7276-85. PubMed PMID: 16024076.
72. Schofield SC, Berno B, Langman M, Hall G, Filiaggi MJ. Gelled calcium polyphosphate matrices delay antibiotic release. *J Dent Res*. 2006 Jul;85(7):643-7. PubMed PMID: 16798866.
73. Dion A, Berno B, Hall G, Filiaggi MJ. The effect of processing on the structural characteristics of vancomycin-loaded amorphous calcium phosphate matrices. *Biomaterials*. 2005 Jul;26(21):4486-94. PubMed PMID: 15701378.
74. Petrone C, Hall G, Langman M, Filiaggi MJ. Compaction strategies for modifying the drug delivery capabilities of gelled calcium polyphosphate matrices. *Acta biomaterialia*. 2008 Mar;4(2):403-13. PubMed PMID: 17997374.
75. Y Kim ML, G Hall, M Filiaggi. Calcium polyphosphate as an anti-cancer drug delivery system. *Journal of Dental Research* 2008.

76. Bray JM, Filiaggi MJ, Bowen CV, Beyea SD. Degradation and drug release in calcium polyphosphate bioceramics: an MRI-based characterization. *Acta biomaterialia*. 2012 Oct;8(10):3821-31. PubMed PMID: 22659178.
77. Cubbery WH. *Tool and Manufacturing Engineers Handbook*. Society of Manufacturing Engineers. 1989:17-36.
78. Dionet CA, Rapp M, Tchirkov A. Comparisons of carboplatin and cisplatin as potentiators of 5-fluorouracil and radiotherapy in the mouse L1210 leukaemia model. *Anticancer research*. 2002 Mar-Apr;22(2A):721-5. PubMed PMID: 12014642.
79. Cipak L, Rauko P, Miadokova E, Cipakova I, Novotny L. Effects of flavonoids on cisplatin-induced apoptosis of HL-60 and L1210 leukemia cells. *Leukemia research*. 2003 Jan;27(1):65-72. PubMed PMID: 12479854.
80. Gonzalez VM, Fuertes MA, Alonso C, Perez JM. Is cisplatin-induced cell death always produced by apoptosis? *Molecular pharmacology*. 2001 Apr;59(4):657-63. PubMed PMID: 11259608.
81. Gibalova L, Seres M, Rusnak A, Ditte P, Labudova M, Uhrik B, et al. P-glycoprotein depresses cisplatin sensitivity in L1210 cells by inhibiting cisplatin-induced caspase-3 activation. *Toxicology in vitro : an international journal published in association with BIBRA*. 2012 Apr;26(3):435-44. PubMed PMID: 22269388.
82. Fujimoto S. Schedule-dependent antitumor activity and toxicity of combinations of 5-fluorouracil and cisplatin/carboplatin against L1210 leukemia-bearing mice. *Biological & pharmaceutical bulletin*. 2006 Nov;29(11):2260-6. PubMed PMID: 17077525.
83. Basu A, Krishnamurthy S. Cellular responses to Cisplatin-induced DNA damage. *Journal of nucleic acids*. 2010;2010. PubMed PMID: 20811617. Pubmed Central PMCID: 2929606.
84. Schuldes H, Bade S, Knobloch J, Jonas D. Loss of in vitro cytotoxicity of cisplatin after storage as stock solution in cell culture medium at various temperatures. *Cancer*. 1997 May 1;79(9):1723-8. PubMed PMID: 9128988.
85. Yi YW, Bae I. Effects of solvents on in vitro potencies of platinum compounds. *DNA repair*. 2011 Nov 10;10(11):1084-5. PubMed PMID: 21978437. Pubmed Central PMCID: 3508678.
86. Arifin DY, Lee LY, Wang CH. Mathematical modeling and simulation of drug release from microspheres: Implications to drug delivery systems. *Advanced drug delivery reviews*. 2006 Nov 30;58(12-13):1274-325. PubMed PMID: 17097189.
87. Filiaggi MJD, N.; Hall, G. A Processing Approach to Tuning the Drug Delivery Characteristics of Calcium Polyphosphate Matrices. *Bioceramics Development and Applications*. 2011;Vol. 1 (doi:10.4303/bda/D101101):4.
88. Viale M, Cafaggi S, Parodi B, Esposito M. Cytotoxicity and cellular accumulation of a new cis-diammineplatinum (II) complex containing procaine in murine L1210 cells sensitive and resistant to cis-diamminedichloroplatinum (II). *Cancer chemotherapy and pharmacology*. 1995;35(5):371-6. PubMed PMID: 7850917.
89. Cipak L, Berczeliova E, Paulikova H. Effects of flavonoids on glutathione and glutathione-related enzymes in cisplatin-treated L1210 leukemia cells. *Neoplasma*. 2003;50(6):443-6. PubMed PMID: 14689067.

